NEOPLASIA
www.neoplasia.com

Volume 11 Number 10 October 2009 pp. 1093–1105 **1093**

CD44v6 Dependence of Premetastatic Niche Preparation by Exosomes[1,2]

Thorsten Jung*, Donatello Castellana*, Pamela Klingbeil*,[3], Ines Cuesta Hernández*, Mario Vitacolonna*, David J. Orlicky†, Steve R. Roffler‡, Pnina Brodt§ and Margot Zöller*

*Department of Tumor Cell Biology, University Hospital of Surgery and German Cancer Research Center, Heidelberg, Germany; †Department of Pathology, University of Colorado Health Sciences Center, Denver, CO, USA; ‡Institute of Biomedical Sciences, Academia Sinica, Taipei, Taiwan; §Department of Surgery, McGill University Health Center, Quebec, Canada

Abstract

The metastasizing capacity of the rat pancreatic adenocarcinoma BSp73ASML (ASML^{wt}) is strikingly reduced by a knockdown of CD44v4-v7 (ASML^{kd}). We used this model to analyze the role of the CD44 variant isoform (CD44v) in (pre)metastatic niche formation. Intrafootpad injections of ASML^{wt}–, but not ASML^{kd}–conditioned medium (CM), strongly promote settlement of ASML^{kd} cells in lymph nodes and lung. Fractionation of CM revealed a contribution by a soluble matrix and exosomes, where the CD44v6-containing ASML^{wt}–soluble fraction can complement ASML^{kd}-exosomes, but not *vice versa*. This implies that exosomes are the final actors, are CD44v-independent, but require a soluble matrix, which depends on CD44v. Analyzing the composition revealed that only the ASML^{wt}-matrix contains c-Met and urokinase-type plasminogen activator receptor. *In vitro*, mostly ASML^{wt}-exosomes promote proliferation and induce gene expression in metastatic organ cells. However, *in vivo* corresponding changes in the (pre) metastatic organ are only observed when both, exosomes plus the soluble matrix, are provided. Thus, neither CD44v nor exosomes alone suffice for (pre)metastatic niche formation. Instead, CD44v suffices for assembling a soluble matrix, which allows exosomes, independent of their origin from poorly or highly metastatic cells, to modulate (pre) metastatic organ cells for tumor cell embedding and growth.

Neoplasia (2009) 11, 1093–1105

Introduction

Metastasis formation relies on an interaction with the primary tumor's surrounding [1], where a small population of cancer-initiating cells (CICs) [2,3] may account for metastasis formation by organizing a niche in the (pre)metastatic organ [3–5], which implies long-distance communication of CIC.

CICs are defined by a set of markers [3,6], one of which, CD44, is expressed in several types of leukemia and carcinoma [7]. CD44 contributes to hematopoietic and leukemic stem cell settlement [8,9]. It plays an important role in leukocyte and metastatic cell motility through hyaluronic acid (HA) binding [10] or association with integrins, cytoskeletal proteins, and metalloproteinases (MMPs) [11–14]. CD44 contributes to stem cell and metastatic cell mobilization by interacting with c-Met [15–17] and protects from apoptosis by interfering with receptor-mediated apoptosis and by activating antiapoptotic proteins [18,19]. Overexpression of CD44v6 promotes metastasis formation [20], which

Abbreviations: ASML^{wt}, BSp73ASML; ASML^{kd}, CD44v4-v7 knockdown in ASML; BMC, bone marrow cell; C3, complement component 3; CD44v, CD44 variant isoform; CIC, cancer-initiating cell; Coll, collagen; CM, conditioned medium; FN, fibronectin; HA, hyaluronic acid; HAS3, HA synthase 3; IFP, intrafootpad; INS-2, intersectin 2; LNC, lymph node cells; LnStr, lymph node stroma cells; LuFb, lung fibroblasts; RAEC, rat aortic endothelial cell line; TSP, thrombospondin; wt, wild type; VN, vitronectin

Address all correspondence to: Margot Zöller, Department Tumor Cell Biology, University Hospital of Surgery, Heidelberg, Im Neuenheimer Feld 365, D-69120 Heidelberg, Germany. E-mail: m.zoeller@dkfz.de

[1]This work was supported by the German Research Foundation, SPP1190, the Mildred-Scheel-Stiftung, and the Tumorzentrum Heidelberg/Mannheim (M.Z.).

[2]This article refers to supplementary materials, which are designated by Tables W1 to W3 and Figures W1 to W3 and are available online at www.neoplasia.com.

[3]Current address: Breakthrough Breast Cancer Research Centre, The Institute of Cancer Research, London, UK.

Received 22 May 2009; Revised 20 June 2009; Accepted 20 June 2009

Copyright © 2009 Neoplasia Press, Inc. All rights reserved 1522-8002/09/$25.00
DOI 10.1593/neo.09822

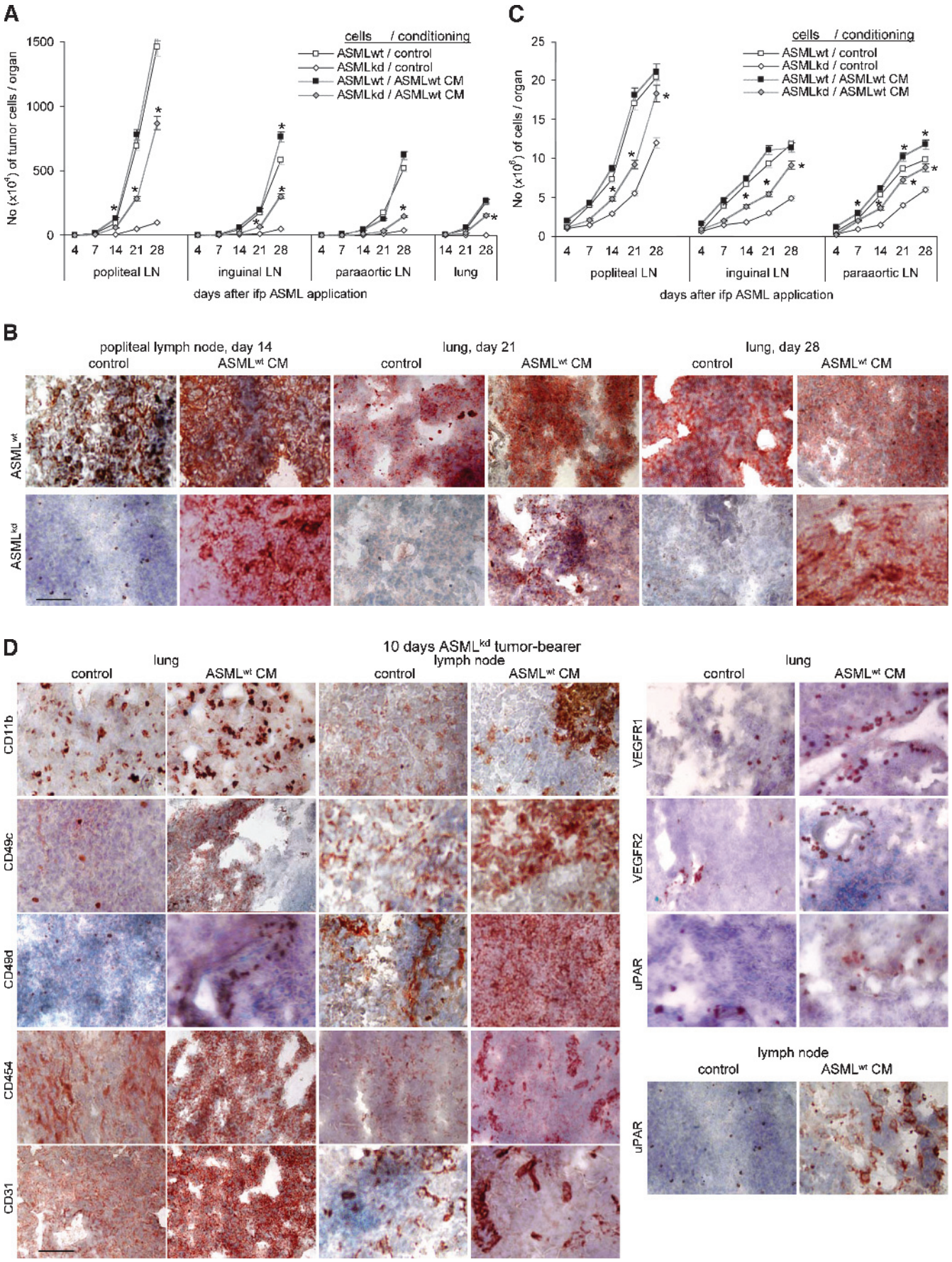
A
No (x10⁴) of tumor cells / organ
cells / conditioning
ASMLwt / control
ASMLkd / control
ASMLwt / ASMLwt CM
ASMLkd / ASMLwt CM
popliteal LN
inguinal LN
paraaortic LN
lung
days after ifp ASML application
C
No (x10⁶) of cells / organ
B
popliteal lymph node, day 14
lung, day 21
lung, day 28
control
ASMLwt CM
ASMLwt
ASMLkd
D
10 days ASMLkd tumor-bearer
lymph node
lung
CD11b
CD49c
CD49d
CD45
CD31
VEGFR1
VEGFR2
uPAR

was confirmed by a selective knockdown of CD44v4-v7 ($ASML^{kd}$) [21] in the highly metastatic BSp73ASML cell line ($ASML^{wt}$) [22].

Settlement of metastasizing tumor cells is facilitated by the establishment of special niches in (pre)metastatic organs [23]. Niche preparation involves stimulation of local fibroblasts by tumor-derived factors and chemokines that attract tumor cells and hematopoietic progenitors [24], lysyl oxidase being important for marrow cell recruitment [25]. Nonetheless, information on long-distance communication between a tumor and the host organs is still limited. We suggest that tumor cells avail special delivery systems and hypothesize that a concerted activity between tumor-derived factors and exosomes is required [26].

Exosomes, small, multivesicular body (MVB)–derived vesicles, are abundantly released by tumor cells on fusion with the plasma membrane [27,28]. Exosomes harbor, besides a common set of membrane and cytosolic molecules, cell type–specific proteins that maintain functional activity [28–30]. Exosomes also contain messenger RNA (mRNA) and microRNA (miRNA) that are transferred to target cells, where they can be translated or mediate RNA silencing [31]. Exosomes function as a potent tool for intercellular communication and gene delivery also in metastasis [28,29].

To prove our hypothesis that tumor-derived factors suffice to promote metastasis formation, we made use of $ASML^{wt}$ and $ASML^{kd}$ cells. $ASML^{wt}$ cells metastasize through the lymphatics to the lung but do not grow locally [22]. $ASML^{kd}$ cells poorly metastasize, which might be a sequel of a defect in a CD44 variant isoform (CD44v)–assembled soluble matrix, which promotes adhesion and apoptosis resistance [21]. Because the ASML tumor does not grow locally, likely because of a defect in angiogenesis induction [22], this model should allow to study the role CD44v takes in creating a metastasis-supporting environment and to define which tumor-derived components suffice for the cross talk between a tumor and the (pre)metastatic organ.

Materials and Methods

Rats and Tumors

Specific pathogen-free BDX rats were fed sterilized food and water *ad libitum*. $ASML^{wt}$ and $ASML^{kd}$ clones of a BDX pancreatic adenocarcinoma [21,22], a BDX lung fibroblast (LuFb), a rat lymph node stroma (LnStr) [32], and a rat aortic endothelial cell line (RAEC) were maintained in RPMI-1640/10% fetal calf serum. Confluent cultures were trypsinized and split.

Antibodies

Primary antibodies are listed in Table W1. Streptavidin-HRP and dye-labeled secondary antibodies were obtained from Dianova, Hamburg, Germany.

Flow Cytometry

Cells ($2\text{-}5 \times 10^5$) were stained according to routine procedures. For intracellular staining, cells were fixed and permeabilized. Samples were processed in a FACSCalibur using the Cell Quest program for analysis (BD, Heidelberg, Germany).

Reverse Transcription–Polymerase Chain Reaction

Total RNA was extracted using TRIzol reagent (Invitrogen, Karlsruhe, Germany). Reverse transcription–polymerase chain reaction followed routine procedures. Primers are listed in Table W2.

Cell and Tissue Preparation

Lymph nodes (LN), femur, and lung were aseptically removed. Bone marrow (BM) was flushed out of the femur, and the lung tissue was cut into small pieces. Tissues were meshed through fine gauze.

Fractionation of Conditioned Medium

Tumor cells were cultured for 24 hours in serum-free medium. The supernatant was collected and centrifuged (10 minutes at 1000*g*, 1500*g*, or 2000*g*). For vesicle depletion, this conditioned medium (CM) was centrifuged for 20 minutes at 10,000*g* and 90 minutes at 26,000*g*. The vesicle-depleted CM is termed "soluble fraction." The soluble fraction contains a strongly adhesive subfraction [21], which was recovered as the plastic adherent fraction after culturing tumor cells for 24 hours in serum-free medium and removing the cells by EDTA treatment. Exosomes were pelleted by centrifugation (64,000*g* for 90 minutes) and resuspended in PBS.

SDS-PAGE and Western Blot

Samples were resolved on 10% SDS-PAGE. Proteins were transferred to nitrocellulose membranes (30 V for 16 hours at 4°C), and membranes were blocked, blotted with streptavidin or primary and HRP-conjugated secondary antibodies (1 hour at room temperature) and developed with the ECL Kit (Amersham Life Sciences, Braunschweig, Germany). For matrix-assisted laser desorption/ionization time-of-flight mass spectrometry (MALDI-TOF) analysis, gels were fixed for 16 hours in 150 ml of ethanol, sensitized for 45 minutes in 0.3 M K-tetrathionate, 0.5 M K-acetate, and 30% ethanol. Gels were washed (H_2O; six times for 10 minutes each) and incubated for 1 hour in 2% silver nitrate. Gels were developed in 0.5 M K-carbonate, 10% Na-thiosulfatepentahydrate, and 0.01% formalin. The reaction was stopped (0.5 M Tris-HCl, 2% acetic acid), and gels were washed (twice for 30 minutes each).

MALDI-TOF Mass Spectrometry

Gels were silver-stained. Protein digestion, sample preparation, MALDI-TOF fingerprint analysis, postsource decay fragmentation analysis, and database searches were performed as described [33].

Histology

Cryostat sections (5-7 μm) of snap-frozen tissue were fixed, stained with the indicated antibodies, washed, and exposed to biotinylated secondary antibodies and alkaline phosphatase–conjugated avidin-biotin

Figure 1. The impact of tumor cell CM on metastasis. (A–C) BDX rats received five daily IFP injections of $ASML^{wt}$-CM or control medium, at day 5 concomitantly with $ASML^{wt}$ or $ASML^{kd}$ cells. Thereafter, medium/CM application was repeated twice per week. Rats were killed 4 to 28 days after tumor cell application. (A) The number of tumor cells ($C4.4A^+$) was evaluated in LN and lung by flow cytometry. Mean values ± SD of three rats per group are shown. (B) Representative examples of tumor cell settlement in LN and lung ($C4.4A^+$) are presented. (C) The mean number ± SD of draining LNC (subtracting the number of tumor cells). (D) Representative examples of LN and lung sections stained with the indicated antibodies are shown. Scale bar: B and D, 0.5 μm. (A and C) Significant differences between rats receiving control medium *versus* CM are indicated by ★. $ASML^{wt}$-CM supports settlement and growth of a weakly metastatic tumor line in draining LNs and lung. $ASML^{wt}$-CM also recruits leukocytes into the draining LNs and promotes leukocyte activation.

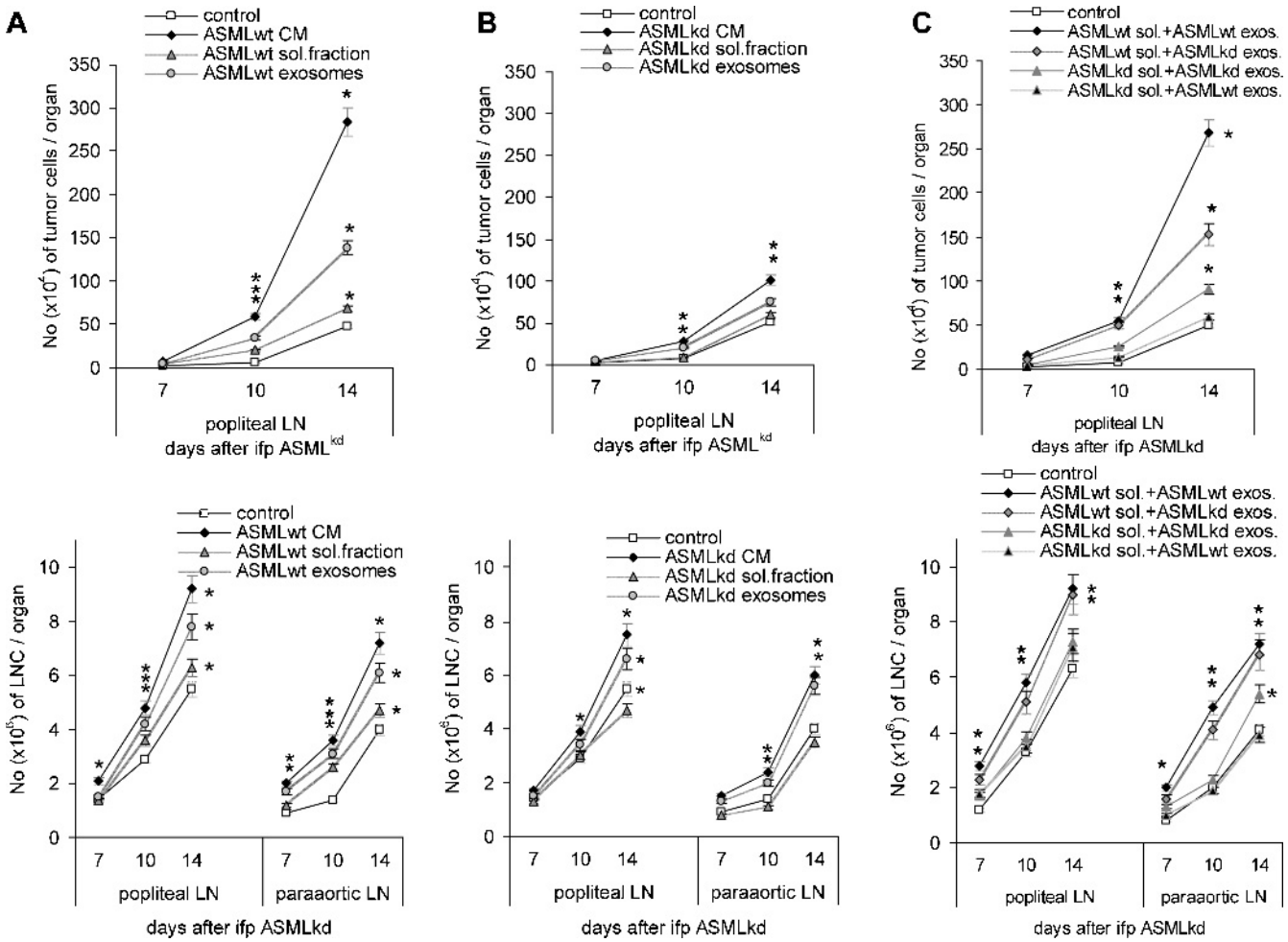

Figure 2. The impact of tumor cell–derived exosomes on metastasis. BDX rats were conditioned as above with control medium, CM, the soluble fraction, or exosomes of (A) ASML^{wt} or (B) ASML^{kd} cells or (C) ASML^{wt}–soluble fraction and ASML^{kd}–soluble fraction and exosome mixtures. At day 5, all rats received ASML^{kd} cells, IFP. Application of CM or fractions thereof was repeated twice per week. Rats were killed 7 to 14 days after tumor cell application. The mean number ± SD of tumor cells (C4.4A^{+}) in the popliteal LN and the number of leukocytes in the popliteal and para-aortic LN (subtracting the number of tumor cells) are shown. Significant differences between rats receiving control medium *versus* CM or fractions thereof are indicated by ★. (D) Summary of the impact of CM and fractions thereof on gene expression in draining LN leukocytes 10 days after tumor cell application. Distinct colors indicate strong and light colors weak up-regulation. The ASML^{wt}–soluble fraction does not suffice for ASML^{kd} tumor cell recruitment into LN and lung and does not initiate activation of draining LN leukocytes. However, the ASML^{wt}–soluble fraction supports exosomes in both metastasis formation and premetastatic organ leukocyte recruitment. This is, albeit less pronounced, also the case for ASML^{kd}-exosomes.

complex solution. Sections were counterstained with hematoxylin. For fluorescence staining of deposited matrix, cells were grown for 48 hours on cover slides. Cells were removed by prolonged EDTA treatment, and slides were blocked and stained with the indicated antibodies and washed and mounted in Elvanol (Sigma Diagnostic, Munic, Germany). Digitized images were generated using a Leica DMRBE microscope (Leica Microsystems, Wetzlar, Germany).

Proliferation Assay

Triplicates of LnStr, LuFb, RAEC (5×10^4) or LN or BM cells (LNCs or BMCs; 2×10^5) were cultured in the presence of CM or fractions thereof. Proliferation was determined after 48 hours by MTT staining.

Apoptosis Induction

Cells were cultured in 96-well plates in RPMI containing cisplatin (*cis*-diamineplatinum(II) dichloride; Sigma, Munich, Germany) and/or CM or fractions thereof. Survival was monitored after 48 hours by annexin V/propidium iodide or evaluation of the percentage of respiratory active cells (MTT assay).

Adhesion Assay

Cells (1×10^6) were suspended in RPMI, CM or fractions thereof and seeded on plastic or adhesive matrix-coated 24-well plates. After 30 minutes at 37°C, nonadherent cells were washed off. Adherent cells were fixed, crystal violet–stained, and lysed. Absorbance was measured at 595 nm. Adhesion is presented as percentage of input cells.

Migration Assay

Cells were seeded in the upper part of a Boyden chamber in 30 μl of RPMI/0.1% BSA. The lower part, separated by an 8-μm (adherent cells) or 5-μm (leukocytes) pore size polycarbonate membrane (Neuroprobe, Gaithersburg, MD), contained 30 μl of RPMI/0.1% BSA, CM,

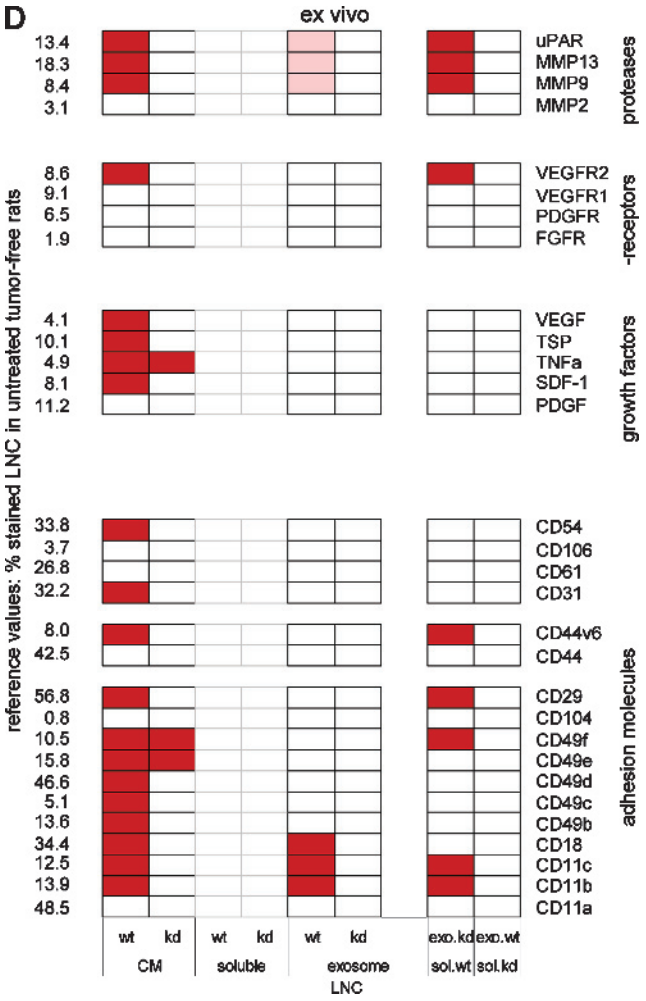

Figure 2. (*continued*).

or fractions thereof. Leukocytes in the lower chamber were counted after 4 hours. Migration of adherent cells was evaluated after 16 hours by staining the lower membrane side with crystal violet. After lysis, OD at 595 nm was measured. Migration is presented as percentage of input cells. In wound healing assays, semiconfluent monolayers were scratched. Medium was changed adding RPMI, CM, or fractions thereof. Migration was documented after 24 to 48 hours by light microscopy.

Zymography

LnStr, LuFb, and RAEC were lysed after overnight culture in the presence of CM or fractions thereof. Lysates, CM, the soluble fraction, or exosomes were incubated with Laemmli buffer (15 minutes at 37°C) and separated in a 10% acrylamide/1 mg/ml gelatin gel. Gels were washed and stained with Coomassie blue.

In Vivo *Assay*

Female rats (10-14 weeks old) received five daily intrafootpad (IFP) injections (150 μg/25 μl) of control medium, CM, or fractions thereof at day 5 concomitantly with tumor cells (1×10^6) and, thereafter, two injections per week. Rats were killed after 4 to 28 days. The popliteal, inguinal, para-aortic, and mesenteric LN, BM, and lung were excised. Tissues were shock frozen or meshed. Animal experiments were approved by the local government authorities.

Statistics

Significance was calculated by the Student's *t* test. *In vitro* assays (triplicates) were repeated three times.

Results

ASML^{wt} CM Supports Metastatic Spread of ASML^{kd} Cells

To explore whether ASML^{wt}-derived soluble factors suffice to prepare a niche that allows embedding and growth of poorly metastatic ASML^{kd} cells, rats received 150 μg of ASML^{wt}-CM, IFP, on five consecutive days, at day 5 concomitantly with ASML^{wt} or ASML^{kd} cells. Thereafter, application of CM was repeated twice per week. Rats were killed, and draining LNs and lung was excised 4 to 28 days after tumor cell application. During this period, a significantly increased number of ASML^{kd} cells were recovered in draining LNs and lung in rats receiving ASML^{wt}-CM. No tumor cells were recovered in the lung of control rats (Figure 1, *A* and *B*). In addition, a higher number of leukocytes were recovered in ASML^{kd}-bearing rats that received ASML^{wt}-CM (Figure 1*C*). In ASML^{wt}-bearing rats, the number of tumor cells and of leukocytes was hardly affected by ASML^{wt}-CM (Figure 1, *A*–*C*). Strongly upregulated expression of CD49c, CD49d, and CD54 and distinctly upregulated expression of urokinase-type plasminogen activator receptor (uPAR) and vascular endothelial growth factor receptors 1 and 2 (VEGFR1 and VEGFR2) are prominent ASML^{wt}-CM–induced alterations in the popliteal LNs and the lung. Unexpectedly, because ASML^{wt} cells hardly induce angiogenesis, LNs contain few but very strongly CD31$^+$ capillaries. CD31 expression is also upregulated in the lung. The most striking feature are CD11b$^+$ clusters in the LNs, which, although smaller, are also seen in the lung (Figure 1*D*).

These data show that ASML^{wt} cells deliver messages that suffice for significant alterations in premetastatic organs, which allow a poorly metastatic cell line to reach, settle, and grow in LNs and the lung. We had shown before that ASML^{wt} cells deliver a soluble matrix, which supports tumor cell adhesion and apoptosis resistance [21], but also that tumor-derived exosomes can exert systemic effects such as angiogenesis induction in tumor-free organs [34]. Because of the large array of activities, which a tumor cell has to fulfill to reach the state of metastatic growth, we considered it unlikely that a single tumor-derived factor sufficed to account for premetastatic niche preparation and hence proceeded to evaluate whether the ASML^{wt}-derived soluble or the vesicular fraction, particularly exosomes, support ASML^{kd} cells in progressing through the metastatic cascade.

An ASML^{wt}–Soluble Fraction Cooperates with Exosomes to Support Metastatic Spread

To examine which components of the ASML^{wt}-CM account for the metastasis-supporting effect, a soluble fraction was separated from exosomes. Settlement of ASML^{kd} cells and leukocyte expansion/recruitment were more efficiently facilitated by ASML^{wt}-exosomes than the soluble fraction. However, neither exosomes nor the soluble fraction reached the efficacy of CM. Because it was apparent that both the soluble fraction and exosomes were required for accelerated metastatic spread, it was of interest whether both fractions must be derived from a metastatic tumor line. The evaluation of tumor cell recruitment into the draining LNs after application of ASML^{kd}-CM, the ASML^{kd}–soluble fraction, or the ASML^{kd}-exosomes revealed that ASML^{kd}-CM and ASML^{kd}-exosomes, but not the soluble fraction, supported, albeit weakly, tumor cell settlement. Applying a mixture of the soluble fraction and exosomes

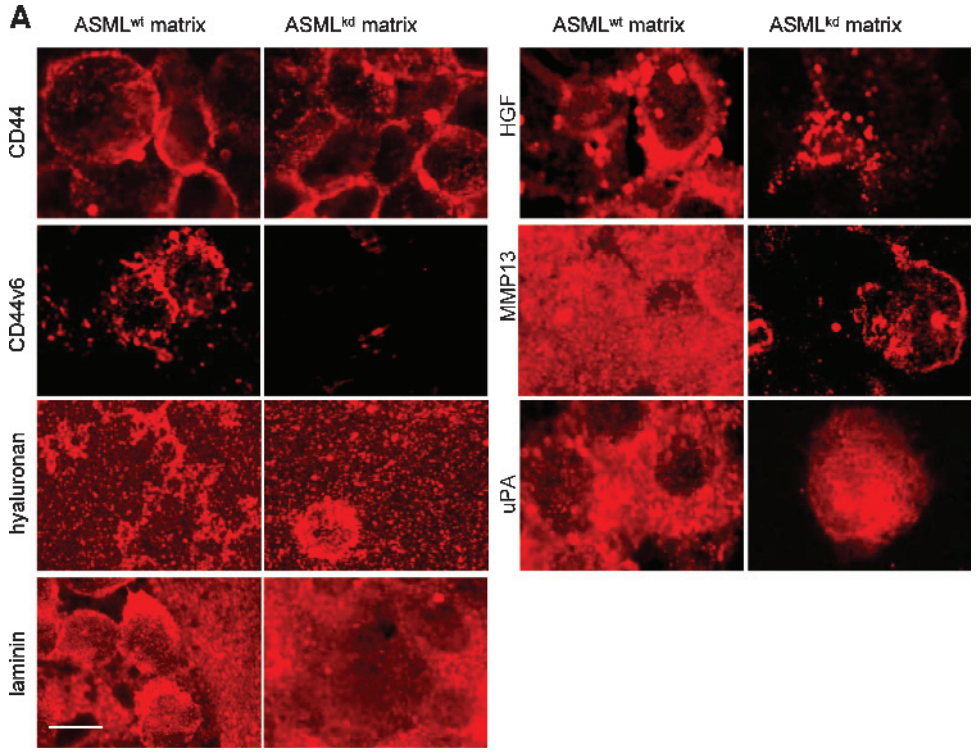
A
ASML^wt matrix
ASML^kd matrix
ASML^wt matrix
ASML^kd matrix
CD44
CD44v6
hyaluronan
laminin
HGF
MMP13
uPA

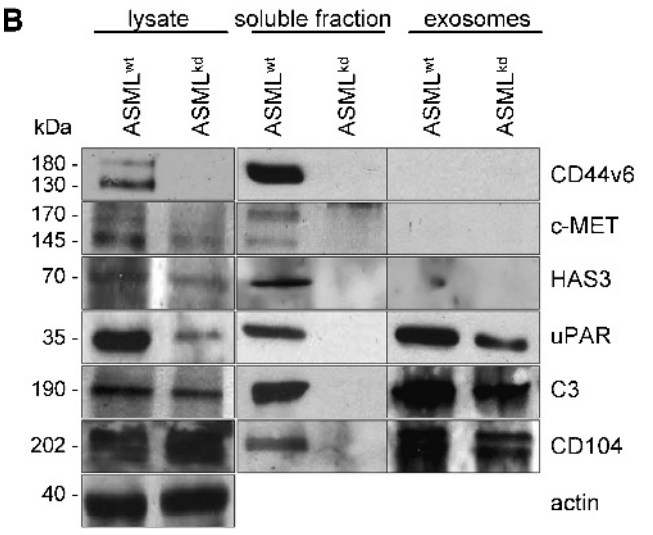
B
lysate
soluble fraction
exosomes
ASML^wt
ASML^kd
kDa
180 -
130 -
170 -
145 -
70 -
35 -
190 -
202 -
40 -
CD44v6
c-MET
HAS3
uPAR
C3
CD104
actin

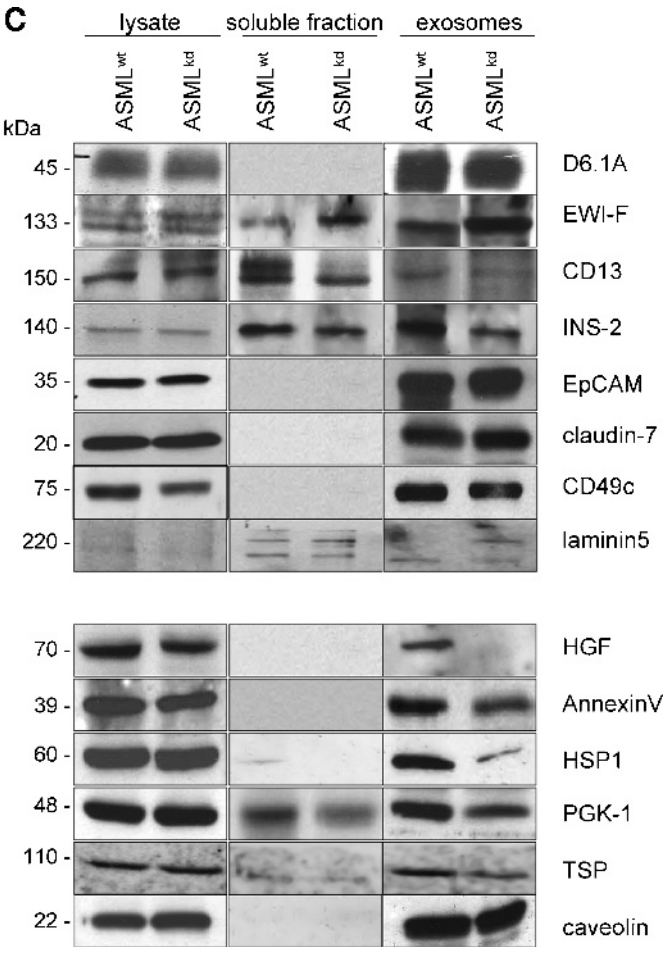
C
lysate
soluble fraction
exosomes
ASML^wt
ASML^kd
kDa
45 -
133 -
150 -
140 -
35 -
20 -
75 -
220 -
D6.1A
EWI-F
CD13
INS-2
EpCAM
claudin-7
CD49c
laminin5
70 -
39 -
60 -
48 -
110 -
22 -
HGF
AnnexinV
HSP1
PGK-1
TSP
caveolin

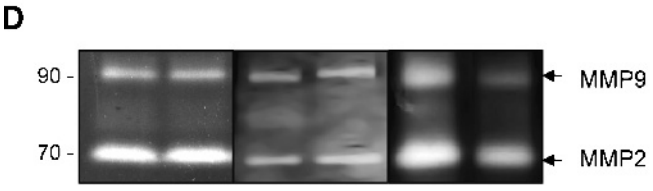
D
90 -
70 -
MMP9
MMP2

from ASML^{wt} and ASML^{kd} cells confirmed that ASML^{kd}-exosomes can cooperate with the ASML^{wt}–soluble fraction (Figure 2, *A–C*).

An *ex vivo* analysis of LNC confirmed a strong effect of ASML^{wt}-CM but only a weak effect of ASML^{kd}-CM on hematopoietic cell activation/expansion in (pre)metastatic organs. The ASML^{wt}–soluble fraction exerted no effect, and exosomes were very weakly effective; that is, CD49b, CD49c, CD49d, stromal-derived factor 1 (SDF-1), MMP9, MMP13, and uPAR expression only becomes stimulated by ASML^{wt}-CM but not by the ASML^{wt}–soluble fraction and slightly by ASML^{wt}-exosomes. However, upregulated gene expression was frequently seen after application of the ASML^{wt}–soluble fraction together with ASML^{kd}-exosomes (Figure 2*D*; examples on the relative increase in marker expression: Figure W1).

Thus, ASML^{wt}-CM creates a milieu that supports metastatic settlement of weakly metastasizing ASML^{kd} cells, but neither the ASML^{wt}–soluble fraction nor the ASML^{wt}-exosomes alone are sufficient. Instead, components of the ASML^{wt}–soluble fraction can cooperate even with ASML^{kd}-exosomes but not *vice versa*. These findings imply that exosomes contain essential messages that require the ASML^{wt}–soluble fraction for delivery. Hence, we examined differences between ASML^{wt} and ASML^{kd} cells, the soluble fraction, and exosomes.

Impact of CD44v on Gene Expression, Protein Secretion/Shedding, and Exosome Delivery

The plastic-deposited matrix of ASML^{wt}, but not ASML^{kd} cells, strongly supports adhesion of both ASML^{wt} and ASML^{kd} cells [21]. This "adhesive" fraction was evaluated for the presence of matrix proteins, growth factors, and proteases frequently deposited in the extracellular matrix. With the exception of a possibly more structured organization of HA in the ASML^{wt}–adhesive fraction, no obvious differences were observed between ASML^{wt}– and ASML^{kd}–matrix proteins. However, hepatocyte growth factor (HGF), MMP13, and uPA were reduced in the ASML^{kd}-matrix. Deposition of other MMPs, platelet-derived growth factor (PDGF), SDF-1, VEGF, and thrombospondin (TSP) was not overtly affected (Figure 3*A* and data not shown).

MALDI-TOF analysis revealed a strong reduction of c-Met and complement component 3 (C3) in the ASML^{kd}–soluble fraction and of annexin II, annexin V, heat shock protein 1 (HSP-1), phosphoglycerate kinase 1 (PGK-1), and monooxygenase activating protein in ASML^{kd}-exosomes.

Western blot confirmed that besides CD44v6, c-Met, uPAR, C3, HA synthase 3 (HAS3), and CD104 were selectively missing in the ASML^{kd}–soluble fraction. C-Met, uPAR, and HAS3 expression was also reduced in ASML^{kd} cells. Instead, C3 and CD104 were missing in the ASML^{kd}–soluble fraction, but expression was not reduced in ASML^{kd} cells (Figure 3*B*).

Exosomes are enriched in tetraspanins, tetraspanin-associated molecules, glycosylphosphatidylinositol-anchored, and other raft-associated molecules [27,29,30]. The recovery of the tetraspanins D6.1A, CD151, CD9 and of the D6.1A-associated molecules F2 alpha receptor regulatory protein, CD13, intersectin 2 (INS-2), epithelial cell adhesion molecule (EpCAM), and EpCAM-associated claudin-7 [27,35], as well as of CD11a, CD49c, CD49f, and CD104 was not or only slightly impaired in ASML^{kd} cells and exosomes. Even the integrin ligands laminin 5 and fibronectin (FN) were partly recovered in exosomes. However, HGF was absent, and recovery of annexin V, HSP-1, PGK-1, and TSP was strongly reduced in ASML^{kd}-exosomes. The expression of these proteins in ASML^{kd} cells was unimpaired (Figure 3*C* and data not shown). Zymography revealed a reduction of MMP9 in ASML^{kd}-exosomes (Figure 3*D*).

Taken together (Table W3), ASML^{wt} cells exhibit several features of pancreatic CICs that are mostly preserved in weakly metastatic ASML^{kd} cells. ASML^{wt} and ASML^{kd} cells express the CIC markers EpCAM, $\alpha_6\beta_4$, CD24, CD133, and CD166 (Figure W2). The recovery of tetraspanins and tetraspanin-associated molecules remained unaltered in ASML^{kd}-exosomes. These findings might explain the metastasis-supporting activity of ASML^{kd}-exosomes. The deficit in HGF could account for the low efficacy of ASML^{kd}-exosomes. Supporting our hypothesis that exosomes are the driving force, but essentially require the soluble fraction, are the deficits of CD44v6, c-Met, uPAR, HAS3, and C3 in the ASML^{kd}–soluble fraction, c-Met, uPAR, and HAS3 even being reduced in ASML^{kd} cells.

Impact of CM on Potential Target Cells

To support our hypothesis for distinct tasks of the soluble fraction and exosomes and their cooperativity in (pre)metastatic niche preparation, we evaluated the impact of the ASML^{wt} and ASML^{kd} soluble fraction and exosomes on adhesion, migration, apoptosis resistance, and proliferation of potential target cells, namely, LnStr, LuFb, RAEC, LNC, and BMC, *in vitro*. In advance, we explored whether the soluble fraction and the exosomes exert a similar impact on adhesion molecule, protease, chemokine/cytokine, and receptor expression on LnStr, LuFb, RAEC, LNC, and BMC *in vivo*.

As expected, the soluble fraction and exosomes influenced gene expression when cocultured with potential target cells. However, distinct to the *ex vivo* analysis, the coculture system revealed that some of the ASML^{wt}-CM–mediated effects are also observed with ASML^{kd}-CM, although less pronounced. Furthermore, both the soluble fraction and exosomes can modulate target cell gene expression *in vitro*. The soluble fraction can influence adhesion molecule expression. Exosomes primarily influence growth factor receptor expression. Exosomes are also involved in the down-regulation of gene expression, mostly of growth factors. As anticipated, not all potential target cells are equally well responsive, and upregulated gene expression differs between distinct target cells. Some CM-mediated effects were seen with neither the soluble fraction nor the exosomes, which indicates that, even allowing

Figure 3. Components of the deposited matrix, the soluble fraction, and exosomes. (A) ASML^{wt} and ASML^{kd} cells were seeded on cover slides. After 48 hours, cells were removed and the matrix was stained with the indicated antibodies and TxR-labeled secondary antibody. Bar, 1.5μm. There is evidence that the ASML^{wt}-adhesive matrix can serve as a store for proteases and growth factors. (B and C) Lysates of ASML^{wt} and ASML^{kd} cells, the soluble fraction, and exosomes were tested by Western blot for the presence of the indicated proteins with emphasis on (B) the soluble fraction and (C) exosomes. ASML^{kd} cells are characterized by a strong to distinct reduction in c-MET, HAS3, uPAR, and C3. These proteins and, in addition, CD104 are absent in the ASML^{kd}–soluble fraction. Recovery of tetraspanin-associated exosomal proteins is mostly unaltered; recovery of some exosomal proteins, not associated with tetraspanins, such as HGF, annexin V, and HSP-1, was reduced in ASML^{kd}-exosomes. (D) Zymography revealed reduced recovery of MMP9 in ASML^{kd}-exosomes.

for direct contact (coculture), target cell activation may require elements from both the soluble fraction and exosomes (Figure 4; detailed information: Figure W3).

These findings confirmed that both the soluble matrix and the exosomes exert an impact on premetastatic organs and that the soluble matrix and the exosomes display distinct activities. In addition, it is important to note that *in vitro* exosomes influenced the expression of a large array of genes, which has not been seen *in vivo*. We interpret the finding in the sense that, *in vivo*, the soluble matrix is required for the delivery of exosomal messages.

Taking that the CM exerted similar effects *in vivo* and *in vitro* and assuming that the less-pronounced effects of separated exosomes *in vivo* compared with *in vitro* are related to inefficient targeting, the *in vitro* coculture system provided a solid basis to search for distinct and joint soluble matrix– and exosome-mediated effects on functional activities of potential target cells.

LnStr, LuFb, and RAEC, but not LNC and BMC, adhered with high efficacy to the ASML^{wt}–adhesive fraction (Figure 5*A*). Thus, the ASML^{wt}–adhesive fraction may particularly attach to tissue stroma and endothelial cells, which could allow delivery of messages and/or exosomes stored within this matrix.

ASML^{wt}-CM and, less efficiently, ASML^{kd}-CM promote LnStr, LuFb, RAEC, and LNC but hardly BMC migration. Migration-promoting activity is restricted to the soluble fraction, whereas exosomes show no effect (Figure 5*B*).

ASML^{wt} cells are highly apoptosis-resistant, and apoptosis resistance is reduced in ASML^{kd} cells [21]. Therefore, we tested for a protective feature of CM on stroma cells. Indeed, ASML^{wt}-CM and the soluble

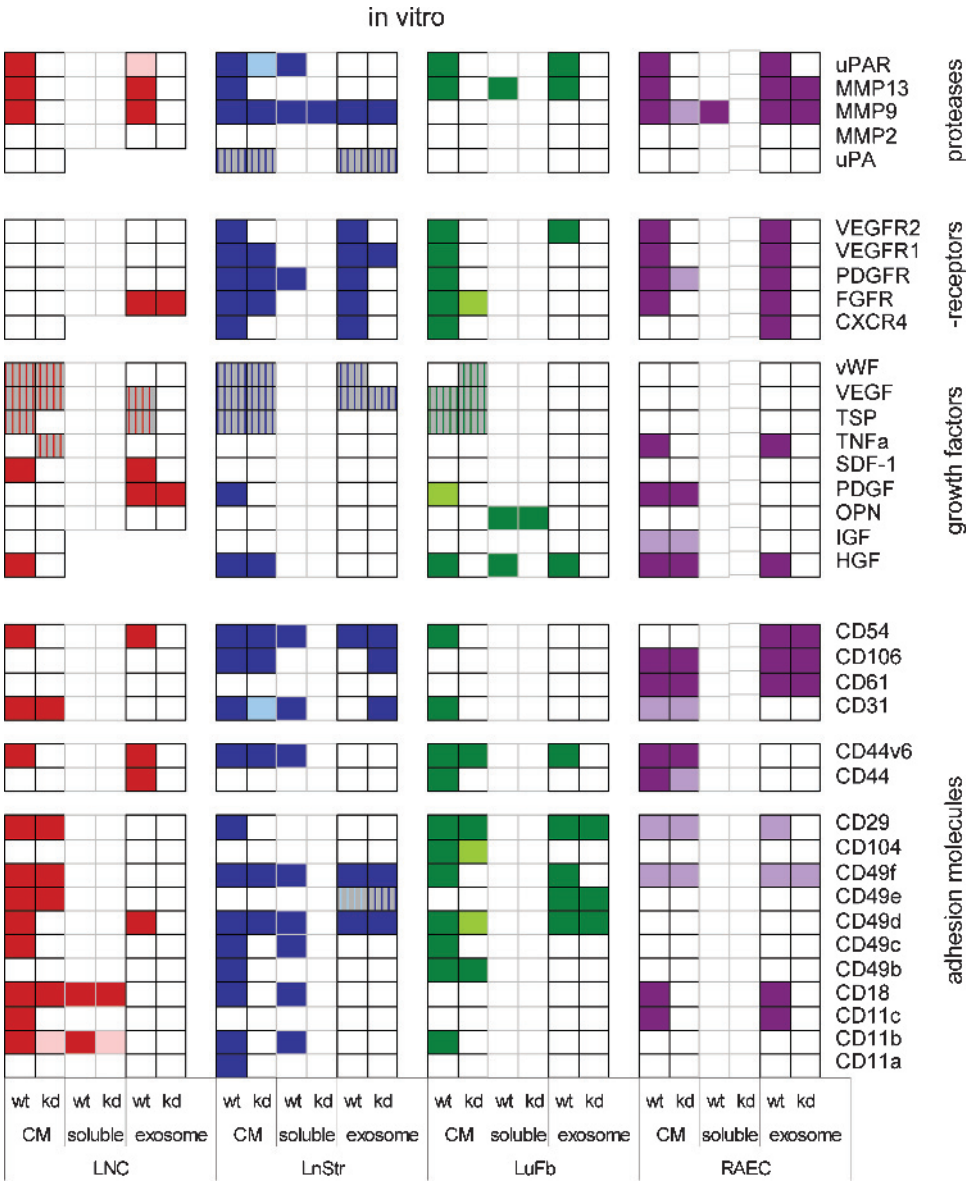

Figure 4. The impact of ASML^{wt}-CM on gene expression in target cells. LNC, LnStr, LuFb, and RAEC were cultured for 48 hours in the presence of ASML^{wt}- and ASML^{kd}-CM or fractions derived thereof. Distinct colors indicate strong and light colors weak up-regulation; stripes indicate downregulated gene expression. In line with the *ex vivo* analysis, ASML^{wt}-CM exerted strong effects on gene expression in potential target cells in the (pre)metastatic organs. Distinct to the *ex vivo* analysis, exosomes exerted some effects *in vitro*, particularly on cytokine receptor and protease expression.

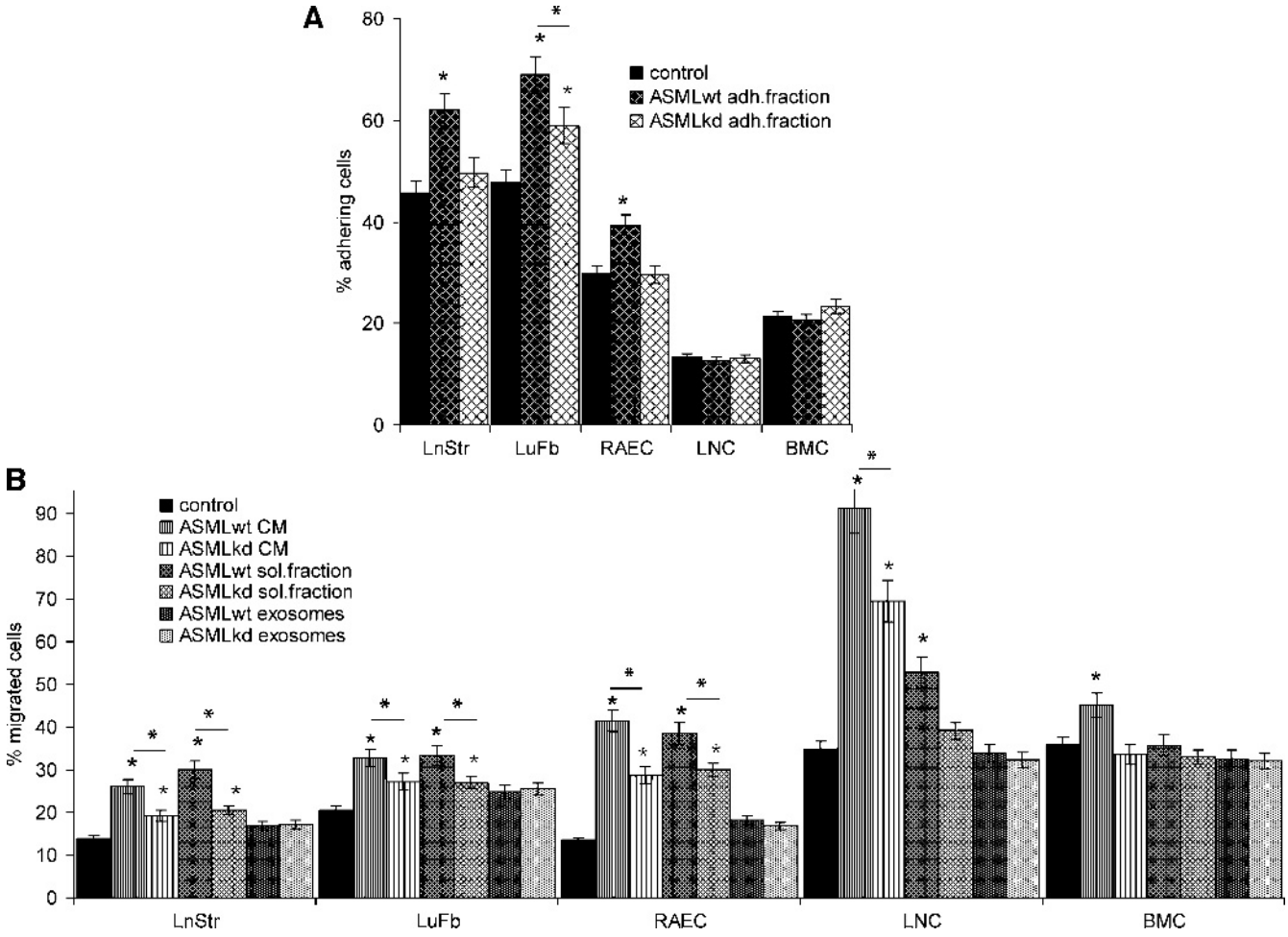

Figure 5. The impact of CM on adhesion and migration. (A) LnStr, LuFb, RAEC, LNC and BMC were seeded in triplicates on flat-bottom 96-well plates coated with medium or the ASML^{wt}- and ASML^{kd}-adhesive matrix. After 30 minutes at 37°C, plates were washed, adherent cells were stained with crystal violet and lysed, and $OD_{595\ nm}$ was evaluated. The percentage of adherent cells is shown. (B) Cells (as in A) were seeded in the upper part of a Boyden chamber. The lower part contained RPMI/0.1% BSA or the indicated fractions. LnStr, LuFb, and RAEC were incubated for 16 hours, whereas LNC and BMC were incubated for 4 hours. LNC and BMC in the lower chamber were counted. LnStr, LuFb, and RAEC at the lower membrane side were crystal violet–stained and lysed, and $OD_{595\ nm}$ was evaluated. Significant differences in comparison to control medium are indicated by ★; significant differences between ASML^{wt}- *versus* ASML^{kd}-CM and fractions thereof are indicated by *. LnStr, LuFb, and RAEC preferentially adhere to the ASML^{wt}–adhesive fraction. These cells and, in addition, LNC migrate toward ASML^{wt}-CM and the ASML^{wt}–soluble fraction.

fraction promote apoptosis resistance of LnStr, LuFb, RAEC, LNC, and BMC. However, a significant increase in cisplatin resistance is only observed in LuFb. Exosomes do not protect from apoptosis (Figure 6, *A* and *B*; data not shown).

C-Met expression is reduced in ASML^{kd} cells and is absent in the ASML^{kd}–soluble fraction. In addition, ASML^{kd}-exosomes do not contain HGF, which could affect cell cycle progression. Indeed, LnStr, LuFb, RAEC, LNC, and BMC proliferate in response to ASML^{wt}-CM, but not ASML^{kd}-CM, and do not proliferate or weakly proliferate in response to the ASML^{kd}–soluble fraction. In LnStr, LuFb, RAEC, and LNC, ASML^{wt}-exosomes but not ASML^{kd}-exosomes induce the strongest response. Notably, culturing cells with a mixture of the ASML^{wt}–soluble fraction and ASML^{kd}-exosomes significantly strengthened proliferative activity (Figure 6*C*). This finding indicated that weak proliferation induction by ASML^{kd}-exosomes cannot exclusively rely on the deficit in HGF. Indeed, proliferation of LnStr and LNC was strongly promoted by HGF, independent of whether the cultures contained ASML^{wt}- or ASML^{kd}-exosomes. Instead, in LuFb, RAEC, and BMC, slightly increased proliferative activity was seen only on coculture with ASML^{kd}-exosomes plus HGF (Figure 6*D*). Thus, besides HGF, additional factors will contribute to the proliferation-supporting activity of ASML^{wt}-exosomes.

The *in vitro* analysis confirmed the superior strength of CM compared with the soluble fraction and exosomes and provided evidence for selective contributions of the soluble fraction *versus* exosomes, which strengthens the *in vivo* observation that preparation of a (pre)metastatic niche depends on cooperative activity of a CD44v-dependent organization of a tumor-derived soluble fraction and exosomes.

Discussion

Metastasis formation can become promoted by a (pre)metastatic niche [1,5,23]. We hypothesized that a single or few soluble factors may not suffice to fulfill the complex demands of the required long-distance cross talk between a tumor and selected (pre)metastatic organs. Instead, exosomes, which transfer proteins, mRNA, and miRNA to selective targets

[27–30], could be suitable candidates. We recently reported that the ASML^{kd} distinct to the ASML^{wt} matrix does not promote tumor cell adhesion and apoptosis resistance *in vitro*. *In vivo*, ASML^{kd} cells have lost the high metastatic capacity of ASML^{wt} cells [21]. Thus, a comparison of ASML^{wt}- *versus* ASML^{kd}-derived factors seemed suited to control our hypothesis. Indeed, ASML^{wt}-CM supports ASML^{kd} metastases. Exosomes play an essential role, however, only when assisted by the ASML^{wt}–soluble fraction.

Consequences of a CD44v^{kd} on CM

The ASML^{wt}–soluble fraction includes an adhesive subfraction, which contains matrix proteins also found in the corresponding ASML^{kd} fraction, which is not adhesive [21]. These striking functional differences may be due to the strongly reduced recovery of HAS3 in the ASML^{kd}–soluble fraction [36] and might be supported by hyaluronidase activity [37], key functions of HA varying considerably with length [36]. The altered assembly of the ASML^{kd}-"nonadhesive" matrix also may account for the reduced recovery of MMP13, uPA, and HGF, where the reduction of the latter two corresponds with the absence of c-Met and uPAR in the soluble fraction and of HGF in ASML^{kd}-exosomes.

CD44v6 has been recovered in the ASML^{wt}–soluble fraction, where differences between ASML^{wt} and ASML^{kd} are most pronounced. The absence of c-Met in the ASML^{kd}–soluble fraction likely is of major importance for reduced metastatic capacity. Activation of c-Met promotes cell survival, supports the epithelial-mesenchymal transition, cell adhesion, and migration, and contributes to angiogenesis [16]. CD44v6 can initiate c-Met activation through HGF binding [17]. Thus, in the absence of CD44v6, c-Met stimulation can become hampered; the consequence of which is reduced transcription of c-Met and c-Met–regulated genes. *UPAR*, one of the c-Met–regulated genes [16,38], is

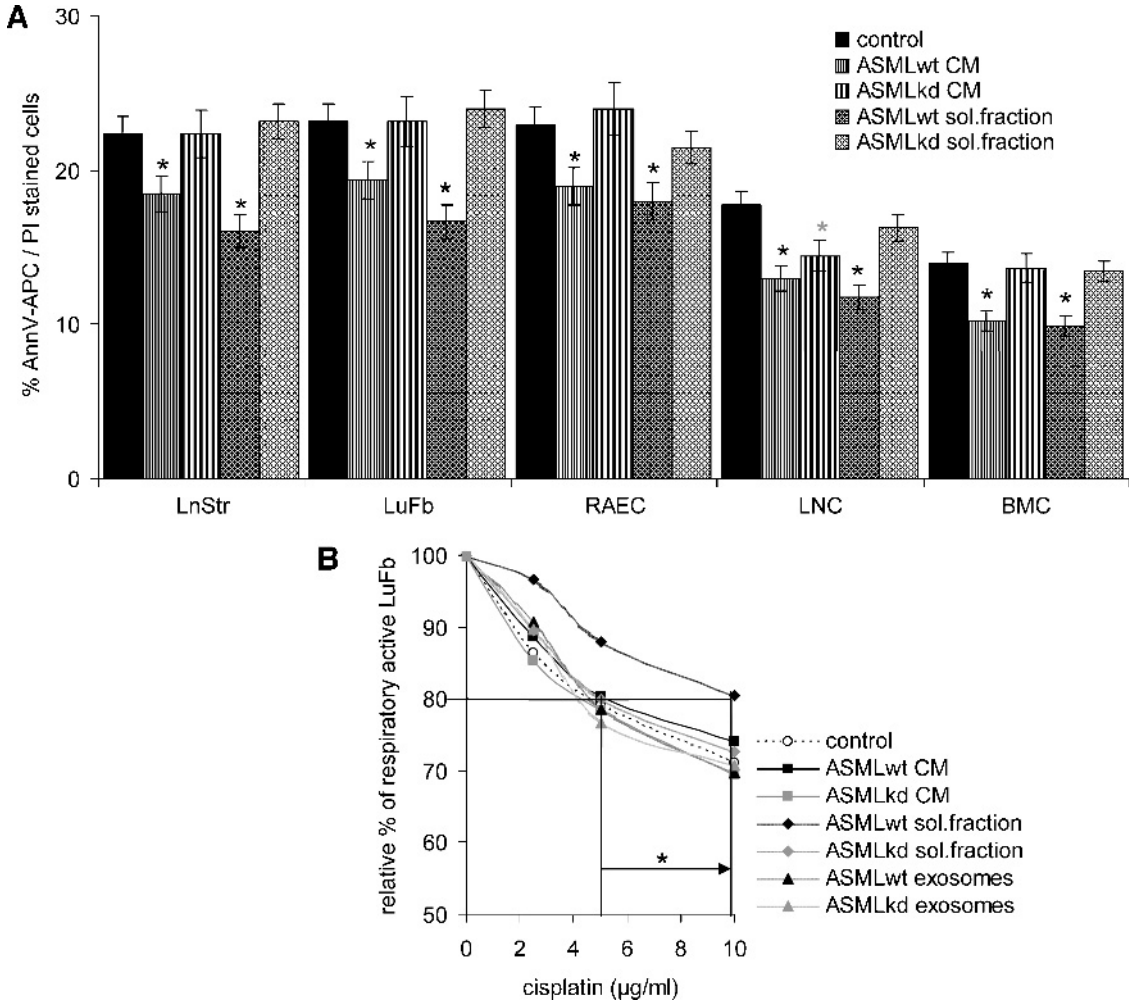

Figure 6. The impact of CM on apoptosis resistance and proliferation. Cells as in Figure 5 were cultured for 48 hours with CM or fractions thereof. (A) The mean percentage ± SD (triplicates) of apoptotic cells (Annexin V–APC/propidium iodide [PI] staining) is shown. (B) LuFb were cultured in the presence of the indicated ASML^{wt} and ASML^{kd} fractions and titrated amounts of cisplatin. The relative percentage (mean ± SD of triplicates) of respiratory active LuFb in comparison to cultures without cisplatin (100%) is shown. (C) The relative increase (mean ± SD of triplicates) in ^{3}H-thymidine incorporation compared with cells cultured in the presence of RPMI/1% BSA is presented. A 1.3-fold increase was considered significant (dashed line). Significant differences in comparison to control medium are indicated by ★; significant differences between ASML^{wt}- *versus* ASML^{kd}-CM and fractions thereof are indicated by *. (D) The relative increase (mean ± SD of triplicates) in ^{3}H-thymidine incorporation in the presence of 5 ng/ml HGF is shown. A significant increase in proliferation by HGF is indicated by ★. ASML^{wt}-CM and the ASML^{wt}–soluble fraction exert a weak apoptosis protective effect on all tested cell lines. Cisplatin resistance was only supported by the ASML^{wt}–soluble fraction. Instead, ASML^{wt}-exosomes support LnStr, LuFb, RAEC, and LNC proliferation.

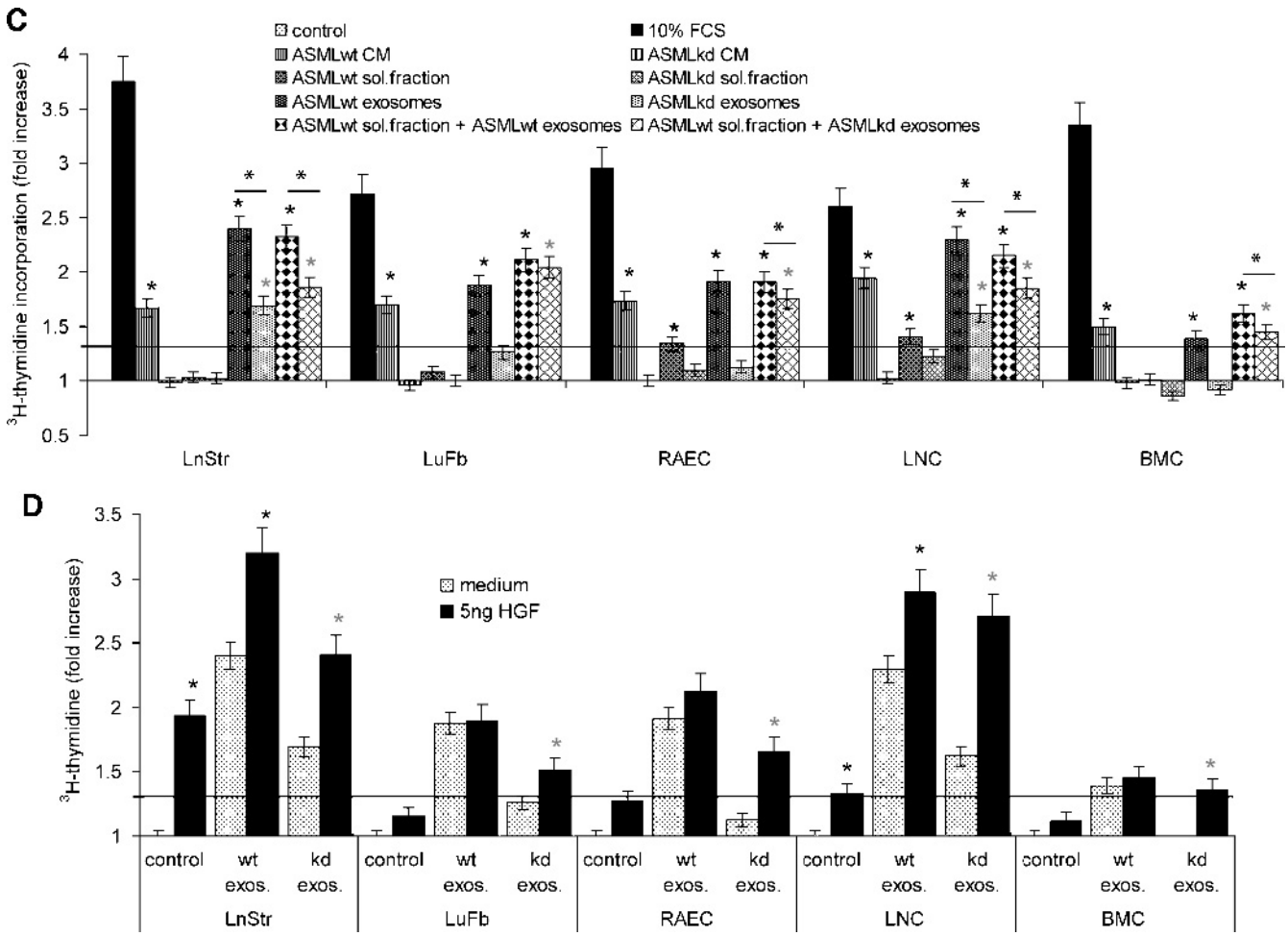

Figure 6. (*continued*).

also strongly downregulated in ASML^{kd} cells and is absent in the soluble fraction. The absence of CD44v6 can contribute to uPAR downregulation, HA binding of CD44 being described to regulate uPAR transcription [39]. UPAR is involved in uPA binding/plasminogen activation and associates with several integrins, epidermal growth factor receptor (EGFR), PDGFR, caveolin, and vitronectin (VN), thereby initiating signal transduction through focal adhesion kinase, Src, Akt, extracellular receptor-activated kinase, and ras [40]. Thus, uPAR could contribute to (pre)metastatic niche preparation by harboring uPA, which is hardly detectable in the ASML^{kd}-adhesive matrix, and/or by binding to integrins or EGFR and initiating signal transduction. In ASML^{wt} cells, CD44v6, c-Met, and uPAR coimmunoprecipitate when cultured in the presence of a chemical cross linker and CD44 cross linking by HA induces c-Met activation (T. Jung, unpublished observations). These observations are in line with the outlined hypothesis and support a central role of CD44v6 in generating a tumor environment that can have a strong impact on premetastatic niche preparation.

C3, although recovered in exosomes, is absent in the ASML^{kd}–soluble fraction. C3a could become important in (pre)metastatic niche preparation as a most potent anaphylatoxin. C3b may recruit exosomes to monocytes through binding to the CD11b receptor [41]. Notably, as also reported for (pre)metastatic niche formation in mammary cancer [25], very strong clusters of CD11b^{+} cells were seen in draining LNs and the lung, which has been suggested to be initiated by tumor-derived chemoattractants S100A8 and S100A9 [42].

These differences in the ASML^{wt}–soluble fraction *versus* the ASML^{kd}–soluble fraction are in line with preferentially the ASML^{wt}–soluble fraction supporting migration and apoptosis resistance of target cells on the way to and within the premetastatic organ. Work is in progress to define the molecular pathways whereby CD44v6 assembles a soluble matrix that supports premetastatic niche formation.

Exosomes can support metastasis formation [43,44]. ASML^{wt}-exosomes, too, distinct to the soluble fraction, exert some effect on premetastatic niche preparation. These effects, albeit weakened, can also be seen with ASML^{kd}-exosomes. Therefore, we suggest that the CD44v^{kd} did not affect exosomal components essential for niche preparation but affected components that strengthened the efficacy of exosomes. In our first trial to separate "essential" from "supporting" exosomal components, we differentiated between exosomes derived from distinct membrane domains.

Recovery of tetraspanins (CD9, CD151, D6.1A) and D6.1A-associated proteins (F2 alpha receptor regulatory protein, CD13, INS-2, CD49c, CD49fCD104, EpCAM, claudin-7) [27] is unimpaired in ASML^{kd}-exosomes. In view of the unaltered tetraspanin web in ASML^{kd}-exosomes, it becomes likely that 1) invagination of caveolae or clathrin-coated pits [25], but not of tetraspanin microdomains, is affected by a CD44v^{kd}, the reasons of which remain to be defined, and 2) TEM-derived exosomes are essential in (pre)metastatic niche preparation. Tetraspanins are known to be involved in fusion processes [27,45] and, thus, could well contribute to the target cell

delivery of exosomes. Unaltered recovery of integrins, including CD11b and integrin ligands (FN and laminin 5) in ASML^{kd}-exosomes, might additionally contribute to their metastasis-supporting activity together with the ASML^{wt}–soluble fraction.

However, the CD44v^{kd} affects the recovery of some non–TEM-associated, likely "supporting" exosomal proteins, whose expression is unaltered in ASML^{kd} cells, which points toward alterations in MVB recruitment: Annexin V binds phosphatidylserine and thereby becomes important in apoptotic signaling [46]. Annexin II is a high-affinity receptor for plasmin and tenascin [47] and can contribute to the integration of tumor-derived exosomes in the soluble tumor matrix. HSPs, including HSP-1, are suggested to activate signaling cascades through binding Toll-like and other receptors [48]. TSP, involved in tumor dormancy by angiogenesis inhibition, also induces a desmoplastic response [49,50]. Monooxygenase activating protein contributes to detoxification of xenobiotics [51]. PGK-1, upregulated in response to oxidative stress, is associated with poor prognosis [52]. Most striking is the absence of HGF in ASML^{kd}-exosomes, which could well contribute to the lower efficacy of ASML^{kd}-exosomes supported by the ASML^{wt}–soluble fraction in premetastatic niche preparation. Although ASML^{wt}-exosomes contain HGF, proliferation of LnStr and LNC was further strengthened by the addition of HGF. This does not exclude an advantage in premetastatic organ cell stimulation by ASML^{wt}-exosome–provided HGF. Furthermore, HGF exerted a stronger effect on LnStr and LNC proliferation and also supported LuFb, RAEC, and BMC proliferation in cocultures with ASML^{kd}-exosomes.

In line with the high recovery of HGF in ASML^{wt}-exosomes, growth factor/receptor expression becomes upregulated in potential targets and proliferation is strongly promoted. Whether this is partly due to exosomal mRNA translation and exosomal miRNA silencing [31] remains to be explored. The former may account for VEGFR expression in non–endothelial cells, the latter for VEGF, von Willebrand factor, and TSP down-regulation. Both phenomena were only seen after coculture with exosomes. The down-regulation of VEGF could explain the very poorly vascularized ASML tumors [22]. Down-regulation of TSP in exosomal target cells could be a compensatory mechanism, and indeed, there has been a striking increase in the vascularization of (pre)metastatic organs after ASML^{wt}-CM treatment. A differential analysis of ASML^{wt} and ASML^{kd} exosomal mRNA and miRNA and selective knockdowns of the most interesting genes in ASML^{wt} cells will allow us to answer these questions. Finally, differences in the responsiveness of potential target cells likely are due to the differences in the activation state of genes in the different cells and/or the selective nature of exosome-target interactions [26,28].

Cooperative Activity of the Soluble Fraction and Exosomes

Metastasis formation of ASML^{kd} cells was strongly promoted by ASML^{wt}-CM and quite efficiently by a mixture of the ASML^{wt}–soluble fraction with ASML^{kd}-exosomes. *Ex vivo* analysis of draining LNC confirmed that no significant changes in marker profiles were induced by the ASML^{wt}–soluble fraction. Exclusively, the ASML^{wt}, but not the ASML^{kd}-exosomes, promoted few changes: most prominently is a higher percentage of CD11b^{+} cells. Instead, ASML^{wt}-CM had a similar impact on protein expression *in vivo* and *in vitro*. These findings imply that exosomes contain essential messages for (pre)metastatic niche preparation, which are not delivered or do not reach the premetastatic organ, except if assisted by the soluble fraction or by the adhesive matrix. The fact that the ASML^{wt}–soluble fraction, which—distinct to the ASML^{kd}–soluble fraction—contains CD44v, c-Met, uPAR and C3, promotes adhesion, migration, and apoptosis resistance *in vitro* and makes an active contribution of the soluble matrix to target activation in the premetastatic organ most likely. The adhesive subfraction may also be a store for exosomes as supported by the recovery of HGF. Reaching the target can become facilitated by proteases, which are more abundant in the ASML^{wt}–soluble fraction. Finally, the adhesive fraction, although not forming a peritumoral matrix, may attach to the lymphatic endothelium, thus serving as a slide bar for exosomes. It should also be noted that the ASML^{wt}-CM/the soluble matrix plus exosome-induced changes in the premetastatic organs correspond well with the features of a premetastatic niche described so far in several murine models. We are currently evaluating the impact of the soluble matrix, in particular that of CD44v, on exosome transport and activity. We will proceed to clarify the mode of interaction of exosomes with target cells on the way to and within premetastatic organs.

In summary, taking advantage of the loss of metastasis formation by a selective CD44v knockdown in a highly metastatic rat pancreatic adenocarcinoma, which does not form a primary tumor, we demonstrate that CD44v is required for the assembly of a soluble matrix that, in cooperation with exosomes, promotes leukocyte, stroma, and endothelial cell activation in the (pre)metastatic organ. Exosomes are the main actors in (pre)metastatic niche preparation. However, exosomes essentially depend on the support of the soluble tumor-derived fraction, which may serve as an exosome carrier and/or a reservoir for growth factors, chemokines, and proteases.

This is the first demonstration that premetastatic niche preparation requires two components, a soluble matrix that supports exosomes in modulating the target cells in the premetastatic organ. It is also the first report to define the activity of CD44v as a cancer initiating cell marker in tumor progression. Although exemplified in an animal model, these findings are demanding to become controlled for their relevance in human cancer progression.

Acknowledgment

Conflict of interest: None of the authors has any conflict of interest.

References

[1] Yilmaz M, Christofori G, and Lehembre F (2007). Distinct mechanisms of tumor invasion and metastasis. *Trends Mol Med* **13**, 535–541.
[2] Regenbrecht CR, Lehrach H, and Adjaye J (2008). Stemming cancer: functional genomics of cancer stem cells in solid tumors. *Stem Cell Rev* **4**, 319–328.
[3] Werbowetski-Ogilvie TE and Bhatia M (2008). Pluripotent human stem cell lines: what we can learn about cancer initiation. *Trends Mol Med* **14**, 323–332.
[4] Alix-Panabières C, Riethdorf S, and Pantel K (2008). Circulating tumor cells and bone marrow micrometastasis. *Clin Cancer Res* **14**, 5013–5021.
[5] Bidard FC, Pierga JY, Vincent-Salomon A, and Poupon MF (2008). A "class action" against the microenvironment: do cancer cells cooperate in metastasis? *Cancer Metastasis Rev* **27**, 5–10.
[6] Clarke MF and Fuller M (2006). Stem cells and cancer: two faces of eve. *Cell* **124**, 1111–1115.
[7] Marhaba R, Klingbeil P, Nübel T, Nazarenko I, Büchler MW, and Zöller M (2008). CD44 and EpCAM: cancer-initiating cell markers. *Curr Mol Med* **8**, 784–804.
[8] Williams DA and Cancelas JA (2006). Leukaemia: niche retreats for stem cells. *Nature* **444**, 827–828.
[9] Khaldoyanidi S (2008). Directing stem cell homing. *Cell Stem Cell* **2**, 198–200.
[10] Toole BP (2004). Hyaluronan: from extracellular glue to pericellular cue. *Nat Rev Cancer* **4**, 528–539.
[11] Marhaba R, Freyschmidt-Paul P, and Zöller M (2006). *In vivo* CD44-CD49d complex formation in autoimmune disease has consequences on T cell activation and apoptosis resistance. *Eur J Immunol* **36**, 3017–3032.
[12] Bourguignon LY (2008). Hyaluronan-mediated CD44 activation of RhoGTPase signaling and cytoskeleton function promotes tumor progression. *Semin Cancer Biol* **18**, 251–259.

[13] Martin TA, Harrison G, Mansel RE, and Jiang WG (2003). The role of the CD44/ezrin complex in cancer metastasis. *Crit Rev Oncol Hematol* **46**, 165–186.
[14] Fjeldstad K and Kolset SO (2005). Decreasing the metastatic potential in cancers—targeting the heparan sulfate proteoglycans. *Curr Drug Targets* **6**, 665–682.
[15] Matzke A, Sargsyan V, Holtmann B, Aramuni G, Asan E, Sendtner M, Pace G, Howells N, Zhang W, Ponta H, et al. (2007). Haploinsufficiency of c-Met in cd44–/– mice identifies a collaboration of CD44 and c-Met *in vivo*. *Mol Cell Biol* **27**, 8797–8806.
[16] Comoglio PM, Giordano S, and Trusolino L (2008). Drug development of MET inhibitors: targeting oncogene addiction and expedience. *Nat Rev Drug Discov* **7**, 504–516.
[17] Orian-Rousseau V and Ponta H (2008). Adhesion proteins meet receptors: a common theme? *Adv Cancer Res* **101**, 63–92.
[18] Ponta H, Sherman L, and Herrlich PA (2003). CD44: from adhesion molecules to signalling regulators. *Nat Rev Mol Cell Biol* **4**, 33–45.
[19] Toole BP and Slomiany MG (2008). Hyaluronan, CD44 and Emmprin: partners in cancer cell chemoresistance. *Drug Resist Updat* **11**, 110–121.
[20] Günthert U, Hofmann M, Rudy W, Reber S, Zöller M, Haussmann I, Matzku S, Wenzel A, Ponta H, and Herrlich P (1991). A new variant of glycoprotein CD44 confers metastatic potential to rat carcinoma cells. *Cell* **65**, 13–24.
[21] Klingbeil P, Marhaba R, Jung T, Ludwig T, and Zöller M (2009). CD44 variant isoforms promote metastasis formation by a tumor cell–matrix crosstalk that supports adhesion and apoptosis resistance. *Mol Cancer Res* **7**, 168–179.
[22] Matzku S, Komitowski D, Mildenberger M, and Zöller M (1983). Characterization of BSp73, a spontaneous rat tumor and its *in vivo* selected variants showing different metastasizing capacities. *Invasion Metastasis* **3**, 109–123.
[23] Bissell MJ and Labarge MA (2005). Context, tissue plasticity, and cancer: are tumor stem cells also regulated by the microenvironment? *Cancer Cell* **7**, 17–23.
[24] Kaplan RN, Riba RD, Zacharoulis S, Bramley AH, Vincent L, Costa C, MacDonald DD, Jin DK, Shido K, Kerns SA, et al. (2005). VEGFR1-positive haematopoietic bone marrow progenitors initiate the pre-metastatic niche. *Nature* **438**, 820–827.
[25] Erler JT, Bennewith KL, Cox TR, Lang G, Bird D, Koong A, Le QT, and Giaccia AJ (2009). Hypoxia-induced lysyl oxidase is a critical mediator of bone marrow cell recruitment to form the premetastatic niche. *Cancer Cell* **15**, 35–44.
[26] Fevrier B and Raposo G (2004). Exosomes: endosomal-derived vesicles shipping extracellular messages. *Curr Opin Cell Biol* **16**, 415–421.
[27] Zöller M (2009). Tetraspanins: push and pull in suppressing and promoting metastasis. *Nat Rev Cancer* **9**, 40–55.
[28] Johnstone RM (2006). Exosomes biological significance: a concise review. *Blood Cells Mol Dis* **36**, 315–321.
[29] Lakkaraju A and Rodriguez-Boulan E (2008). Itinerant exosomes: emerging roles in cell and tissue polarity. *Trends Cell Biol* **18**, 199–209.
[30] Gruenberg J and Stenmark H (2004). The biogenesis of multivesicular endosomes. *Nat Rev Mol Cell Biol* **5**, 317–323.
[31] Zakharova L, Svetlova M, and Fomina AF (2007). T cell exosomes induce cholesterol accumulation in human monocytes via phosphatidylserine receptor. *J Cell Physiol* **212**, 174–181.
[32] LeBedis C, Chen K, Fallavollita L, Boutros T, and Brodt P (2002). Peripheral lymph node stromal cells can promote growth and tumorigenicity of breast carcinoma cells through the release of IGF-I and EGF. *Int J Cancer* **100**, 2–8.
[33] Gobom J, Schuerenberg M, Mueller M, Theiss D, Lehrach H, and Nordhoff E (2001). α-Cyano-4-hydroxycinnamic acid affinity sample preparation. A protocol for MALDI-MS peptide analysis in proteomics. *Anal Chem* **73**, 434–438.
[34] Gesierich S, Berezovskiy I, Ryschich E, and Zöller M (2006). Systemic induction of the angiogenesis switch by the tetraspanin D6.1A/CO-029. *Cancer Res* **66**, 7083–7094.
[35] Schmidt DS, Klingbeil P, Schnölzer M, and Zöller M (2004). CD44 variant isoforms associate with tetraspanins and EpCAM. *Exp Cell Res* **297**, 329–347.
[36] Stern R, Asari AA, and Sugahara KN (2006). Hyaluronan fragments: an information-rich system. *Eur J Cell Biol* **85**, 699–715.
[37] Girish KS and Kemparaju K (2007). The magic glue hyaluronan and its eraser hyaluronidase: a biological overview. *Life Sci* **80**, 1921–1943.
[38] Lee KH, Choi EY, Hyun MS, Jang BI, Kim TN, Lee HJ, Eun JY, Kim HG, Yoon SS, Lee DS, et al. (2008). Role of hepatocyte growth factor/c-Met signaling in regulating urokinase plasminogen activator on invasiveness in human hepatocellular carcinoma: a potential therapeutic target. *Clin Exp Metastasis* **25**, 89–96.
[39] Kobayashi H, Suzuki M, Kanayama N, Nishida T, Takigawa M, and Terao T (2002). CD44 stimulation by fragmented hyaluronic acid induces upregulation of urokinase-type plasminogen activator and its receptor and subsequently facilitates invasion of human chondrosarcoma cells. *Int J Cancer* **102**, 379–389.
[40] Mazar AP (2008). Urokinase plasminogen activator receptor choreographs multiple ligand interactions: implications for tumor progression and therapy. *Clin Cancer Res* **14**, 5649–5655.
[41] Wysoczynski M, Ratajczak J, Reca R, Kucia M, and Ratajczak MZ (2007). The third complement component as modulator of platelet production. *Adv Exp Med Biol* **598**, 226–239.
[42] Hiratsuka S, Watanabe A, Sakurai Y, Akashi-Takamura S, Ishibashi S, Miyake K, Shibuya M, Akira S, Aburatani H, and Maru Y (2008). The S100A8-serum amyloid A3-TLR4 paracrine cascade establishes a pre-metastatic phase. *Nat Cell Biol* **10**, 1349–1355.
[43] Janowska-Wieczorek A, Wysoczynski M, Kijowski J, Marquez-Curtis L, Machalinski B, Ratajczak J, and Ratajczak MZ (2005). Microvesicles derived from activated platelets induce metastasis and angiogenesis in lung cancer. *Int J Cancer* **113**, 752–760.
[44] Hao S, Ye Z, Li F, Meng Q, Qureshi M, Yang J, and Xiang J (2006). Epigenetic transfer of metastatic activity by uptake of highly metastatic B16 melanoma cell–released exosomes. *Exp Oncol* **28**, 126–131.
[45] Rubinstein E, Ziyyat A, Wolf JP, Le Naour F, and Boucheix C (2006). The molecular players of sperm-egg fusion in mammals. *Semin Cell Dev Biol* **17**, 254–263.
[46] Reutelingsperger CP and van Heerde WL (1997). Annexin V, the regulator of phosphatidylserine-catalyzed inflammation and coagulation during apoptosis. *Cell Mol Life Sci* **53**, 527–532.
[47] Sharma MC and Sharma M (2007). The role of annexin II in angiogenesis and tumor progression: a potential therapeutic target. *Curr Pharm Des* **13**, 3568–3575.
[48] Cappello F, de Macario EC, Marasà L, Zummo G, and Macario AJ (2008). Hsp60 expression, new locations, functions and perspectives for cancer diagnosis and therapy. *Cancer Biol Ther* **7**, 801–809.
[49] Kazerounian S, Yee KO, and Lawler J (2008). Thrombospondins in cancer. *Cell Mol Life Sci* **65**, 700–712.
[50] Kang SY and Watnick RS (2008). Regulation of tumor dormancy as a function of tumor-mediated paracrine regulation of stromal Tsp-1 and VEGF expression. *APMIS* **116**, 638–647.
[51] Standop J, Ulrich AB, Schneider MB, Büchler MW, and Pour PM (2002). Differences in the expression of xenobiotic-metabolizing enzymes between islets derived from the ventral and dorsal anlage of the pancreas. *Pancreatology* **2**, 510–518.
[52] Jang CH, Lee IA, Ha YR, Lim J, Sung MK, Lee SJ, and Kim JS (2008). PGK1 induction by a hydrogen peroxide treatment is suppressed by antioxidants in human colon carcinoma cells. *Biosci Biotechnol Biochem* **72**, 1799–1808.

Table W1. List of Antibodies.

Antibody	Supplier
$\alpha_6\beta_4$	Clone B5.5 [1]
Actin	BD, Heidelberg, G.
Annexin V	Santa Cruz, Heidelberg, G.
β-Catenin	BD, Heidelberg, G.
bFGF	Oncogene, Boston, MA
C3	MP Biomed., Eschwege, G.
C4.4A	Clone C4.4 [1]
Caveolin	BD, Heidelberg, G.
CD44s	Clone Ox50 (EAACC)
CD44v6	Clone A2.6 [1]
CD104	BD, Heidelberg, G.
CD106	Biozol, Eching, G.
CD11a	BD, Heidelberg, G.
CD11b	Clone Ox42 (EAACC)
CD11c	Clone Ox41 (EAACC)
CD13	[2]
CD133	Abcam, Cambridge, UK
CD151	[3]
CD18	BD, Heidelberg, G.
CD24	Santa Cruz, Heidelberg, G.
CD29	BD, Heidelberg, G.
CD31	BD, Heidelberg, G.
CD49a	BD, Heidelberg, G.
CD49b	BD, Heidelberg, G.
CD49c	BD, Heidelberg, G.
CD49d	BD, Heidelberg, G.
CD49e	BD, Heidelberg, G.
CD49f	Abcam, Cambridge, UK
CD53	BD, Heidelberg, G.
CD54	Biozol, Eching, G.
CD61	Biozol, Eching, G.
CD81	Santa Cruz, Heidelberg, G.
CD9	BD, Heidelberg, G.
Claudin-7	[4]
c-Met	New England Biolabs, Frankfurt, G.
Collagen I	Rockland, Gilbertsville, PA
Collagen II	LabVision, Fremont, CA
Collagen III	ARB, Golden, CO
Collagen IV	Rockland, Gilbertsville, PA
D6.1A	Clone D6.1 [1]
EpCAM	Clone D5.7 [1]
EWI-F	[5]
EGFR	Santa Cruz, Heidelberg, G.
FN	BD, Heidelberg, G.
Galectin	Santa Cruz, Heidelberg, G.
HAS3	Abcam, Cambridge, UK
HSP-1	Santa Cruz, Heidelberg, G.
Hyaluronan	Rockland, Gilbertsville, PA
INS-2	Santa Cruz, Heidelberg, G.
Laminin 1	Rockland, Gilbertsville, PA
Laminin 5	BD, Heidelberg, G.
MMP13	Dianova, Hamburg, G.
MMP2	Dianova, Hamburg, G.
MMP9	Dianova, Hamburg, G.
Osteopontin	Santa Cruz, Heidelberg, G.
PDGF	BD, Heidelberg, G.
PDGFR	BD, Heidelberg, G.
PGK-1	Santa Cruz, Heidelberg, G.
S100A4	Abcam, Cambridge, UK
SDF-1	Abcam, Cambridge, UK
Tenascin	LabVision, Fremont, CA
TGFβ	Santa Cruz, Heidelberg, G.
Thrombospondin	Santa Cruz, Heidelberg, G.
TNFα	BD, Heidelberg, G.
uPA	Calbiochem, Darmstadt, G.
uPAR	Calbiochem, Darmstadt, G.
VEGF	Biotrend, Köln, G.
VEGFR1	Biotrend, Köln, G.
VEGFR2	Biotrend, Köln, G.
VN	Biotrend, Köln, G.
vWF	Abcam, Cambridge, UK

CD44s indicates CD44 standard isoform; *EAACC*, European Association of Animal Cell Cultures, Porton Down, UK; *G.*, Germany.

References

[1] Matzku S, Wenzel A, Liu S, and Zöller M (1989). Antigenic differences between metastatic and nonmetastatic rat tumor variants characterized by monoclonal antibodies. *Cancer Res* **49**, 1294–1299.

[2] Chang YW, Chen SC, Cheng EC, Ko YP, Lin YC, Kao YR, Tsay YG, Yang PC, Wu CW, and Roffler SR (2005). CD13 (aminopeptidase N) can associate with tumor-associated antigen L6 and enhance the motility of human lung cancer cells. *Int J Cancer* **116**, 243–252.

[3] Claas C, Wahl J, Orlicky D, Karaduman H, Schnölzer M, Kempf T, and Zöller M (2005). The tetraspanin D6.1A and its molecular partners on rat carcinoma cells. *Biochem J* **389**, 99–110.

[4] Langbein L, Pape UF, Grund C, Kuhn C, Prätzel S, Moll I, Moll R, and Franke WW (2003). Tight junction–related structures in the absence of a lumen: occludin, claudins and tight junction plaque proteins in densely packed cell formations of stratified epithelia and squamous cell carcinomas. *Eur J Cell Biol* **82**, 385–400.

[5] Orlicky DJ, Lieber JG, Morin CL, and Evans RM (1998). Synthesis and accumulation of a receptor regulatory protein associated with lipid droplet accumulation in 3T3-L1 cells. *J Lipid Res* **39**, 1152–1161.

Table W2. List of Primers.

The following primers were used	
CD133	
Sense	5′-AGCCAAGACACCTTCAATGC-3′
Antisense	5′-ACGGTGTTGAGTTCCCTGTC-3′
CD166	
Sense	5′-AACCTGGAGAGTCAGGAGCA-3′
Antisense	5′-TGCGAGCTGTGATTTGTTTC
CD24	
Sense	5′-ACATCGGTTGCACCATTTTC-3′
Antisense	5′-GAGAGAGAGGGCCAGGAGAC-3′
GADPH	
Sense	5′-GACCCCTTCATTGACCTCAAC-3′
Antisense	5′-CTTCTCCATGGTGGTGAAGAC-3′

Amplification was performed for 30 cycles starting with 1 μg of complementary DNA. Annealing temperatures have been as follows: CD133, 57°C; CD24 and CD166, 60°C; and GAPDH, 55°C. Polymerase chain reaction products were separated by electrophoresis in a 1.5% agarose gel.

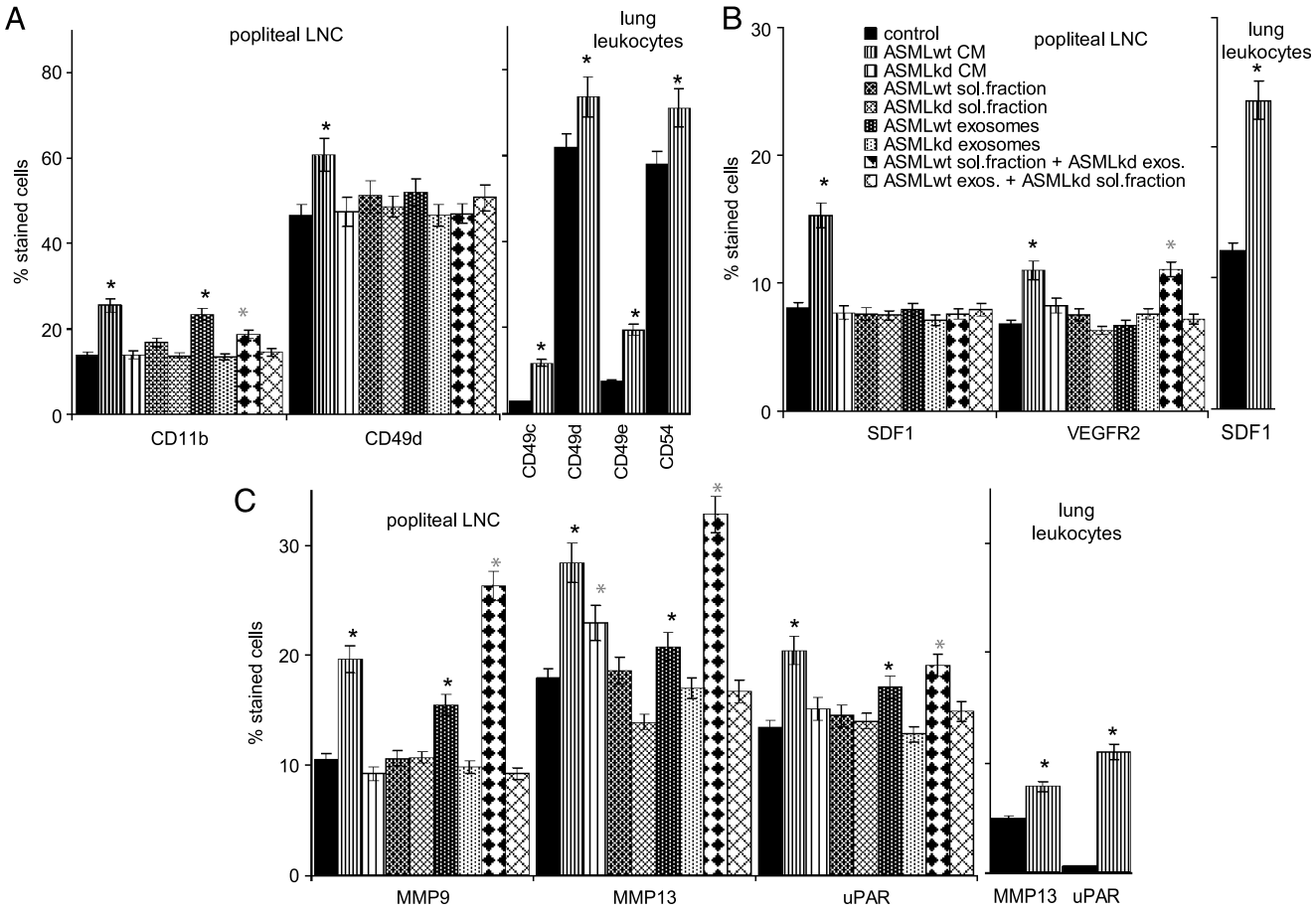

Figure W1. The impact of ASML^{wt}-CM on gene expression in target cells. BDX rats received ASML^{wt}- or ASML^{kd}-CM or fractions thereof and thereafter ASML^{kd} cells as described in Figure 1. LN and lung leukocytes were isolated. Expression of (A) integrins, (B) chemokines, chemokine receptors, and (C) matrix degrading enzymes was evaluated by flow cytometry. The percentage of stained cells (mean ± SD of three experiments) is shown. Significant differences between control medium *versus* CM and fractions thereof are indicated by ★; significant differences between ASML^{wt}- *versus* ASML^{kd}-CM and fractions thereof are indicated by *.

Table W3. ASML^{wt} *Versus* ASML^{kd} Cells: Protein Expression and Recovery in the Soluble Matrix and in Exosomes.

Marker	Cells	Soluble Fraction	Exosomes
	wt/kd	wt/kd	wt/kd
Metastasis markers			
CD44	+/+	nt/nt	nt/nt
CD44v6	+++/−−	+++/−−	−−/−−
EpCAM	+++/+++	−−/−−	+++/+++
CD133	±/±	nt/nt	nt/nt
CD166	±/±	nt/nt	nt/nt
C4.4A	+++/+++	−−/−−	+++/+++
$\alpha_6\beta_4$	+++/++	+/−−	+++/+++
CD24	+/+	−−/−−	+/+
S100A4	++/++	−−/−−	++/++
Matrix proteins			
Coll I	++/++	++/++	nt/nt
Coll II	++/++	++/++	nt/nt
Coll III	+/+	+/+	nt/nt
Coll IV	++/++	++/++	nt/nt
FN	++/++	++/++	±/±
Galectin 3	+++/+++	+++/+++	nt/nt
HA	+++/+++	+++/+++	nt/nt
LN1	+++/+++	+++/+++	nt/nt
LN5	+++/+++	++/++	+/+
Tenascin	++/++	++/++	nt/nt
VN	++/++	++/++	nt/nt
Adhesion molecules			
CD11a	+/+	±/±	+/+
CD11b	+/+	−−/−−	+/+
CD11c	+/+	−−/−−	+/+
CD18	+/+	±/±	+/+
CD29	+++/+++	+/+	+++/+++
CD49b	+/+	−−/−−	+/+
CD49c	+/±	−−/−−	++/++
CD49d	±/±	−−/−−	±/±
CD49e	+/+	±/±	+/+
CD49f	++/++	−−/−−	++/++
CD61	±/±	−−/−−	nt/nt
CD104	+++/+++	+/−−	+++/+++
Enzymes and receptors			
uPA	++/++	nt/nt	nt/nt
uPAR	+++/±	++/−−	+++/++
MMP2	++/++	+/+	++/++
MMP9	+/+	+/+	+/±
MMP13	+/+	−−/−−	+/+
CD13	++/++	++/+	++/++
HAS3	++/+	++/−−	−−/−−
PGK-1	+++/+++	+/+	++/±
Tetraspanins			
CD9	+++/+++	++/++	+++/+++
CD81	+++/+++	−−/−−	+++/+++
CD151	++/++	++/++	+++/+++
D6.1A	+++/+++	−−/−−	+++/+++
Cytokines and receptors			
HGF	++/++	−−/−−	++/−−
PDGF	+/+	nt/nt	nt/nt
SDF-1	+/+	+/+	nt/nt
VEGF	+/+	+/+	nt/nt
OPN	+/+	−−/−−	−−/−−
TSP	++/++	±/±	++/+
c-Met	++/±	++/−−	−−/−−
VEGFR1	+/+	nt/nt	nt/nt
VEGFR2	+/+	nt/nt	nt/nt
Others			
C3	++/++	++/−−	++/++
Annexin II	++/++	−−/−−	++/−−
Annexin V	++/++	−−/−−	++/+
HSP-1	+++/+++	−−/−−	+++/±
Caveolin	+++/+++	−−/−−	+++/+++
EWI-F	++/++	±/±	++/++
INS-2	++/++	+/+	++/++
Claudin-7	+++/+++	−−/−−	+++/+++

Coll indicates collagen; *kd*, knock down; *wt*, wild type; −−, negative; ±, weak; +, distinct; ++, strong; +++, very strong; *nt*, not tested.

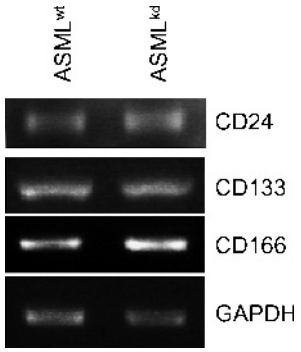

Figure W2. CIC marker expression in ASML^{wt} and ASML^{kd} cells. Expression of the CIC markers CD24, CD133, and CD166 in ASML^{wt} and ASML^{kd} cells was evaluated by reverse transcription–polymerase chain reaction. These markers are expressed by both ASML^{wt} and ASML^{kd} cells.

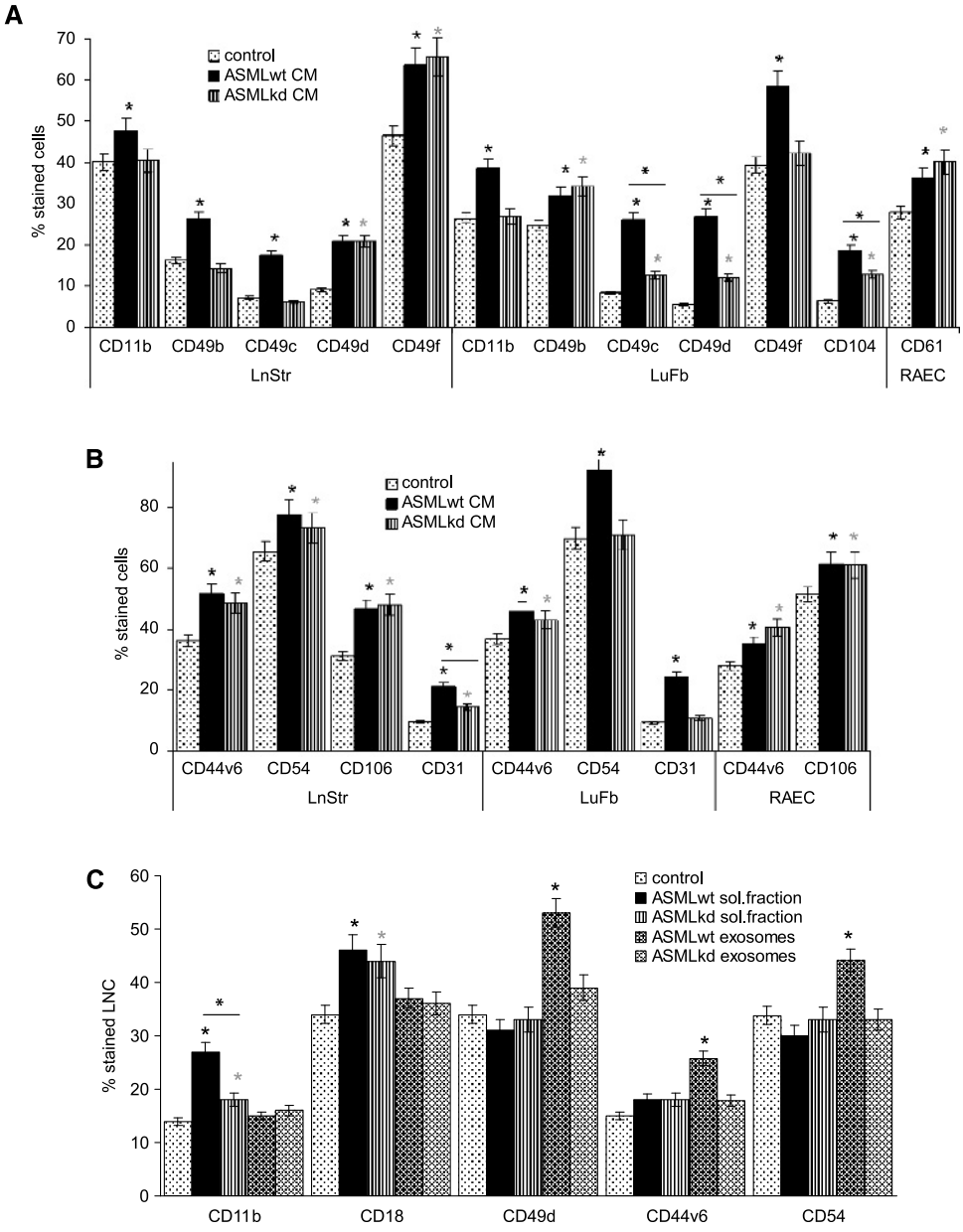

Figure W3. Modulated gene expression by ASML^{wt}–conditioned medium. (A, B, D, E, and F) LnStr, LuFb, and RAEC were cultured for 48 hours in the presence of ASML^{wt}- and ASML^{kd}-CM. (C) LNC and (G) LnStr, LuFb, and RAEC were cultured for 48 hours in the presence of ASML^{wt}– and ASML^{kd}–soluble fraction or exosomes. Cells were harvested, and the expression of (A–C) adhesion molecules and (D and E) cytokines/chemokines and receptors and (F and G) matrix degrading enzymes was evaluated by flow cytometry. Mean values ± SD of three experiments are shown. Significant differences in comparison the control medium are indicated by ★; significant differences between ASML^{wt}- *versus* ASML^{kd}-CM and fractions thereof are indicated by *.

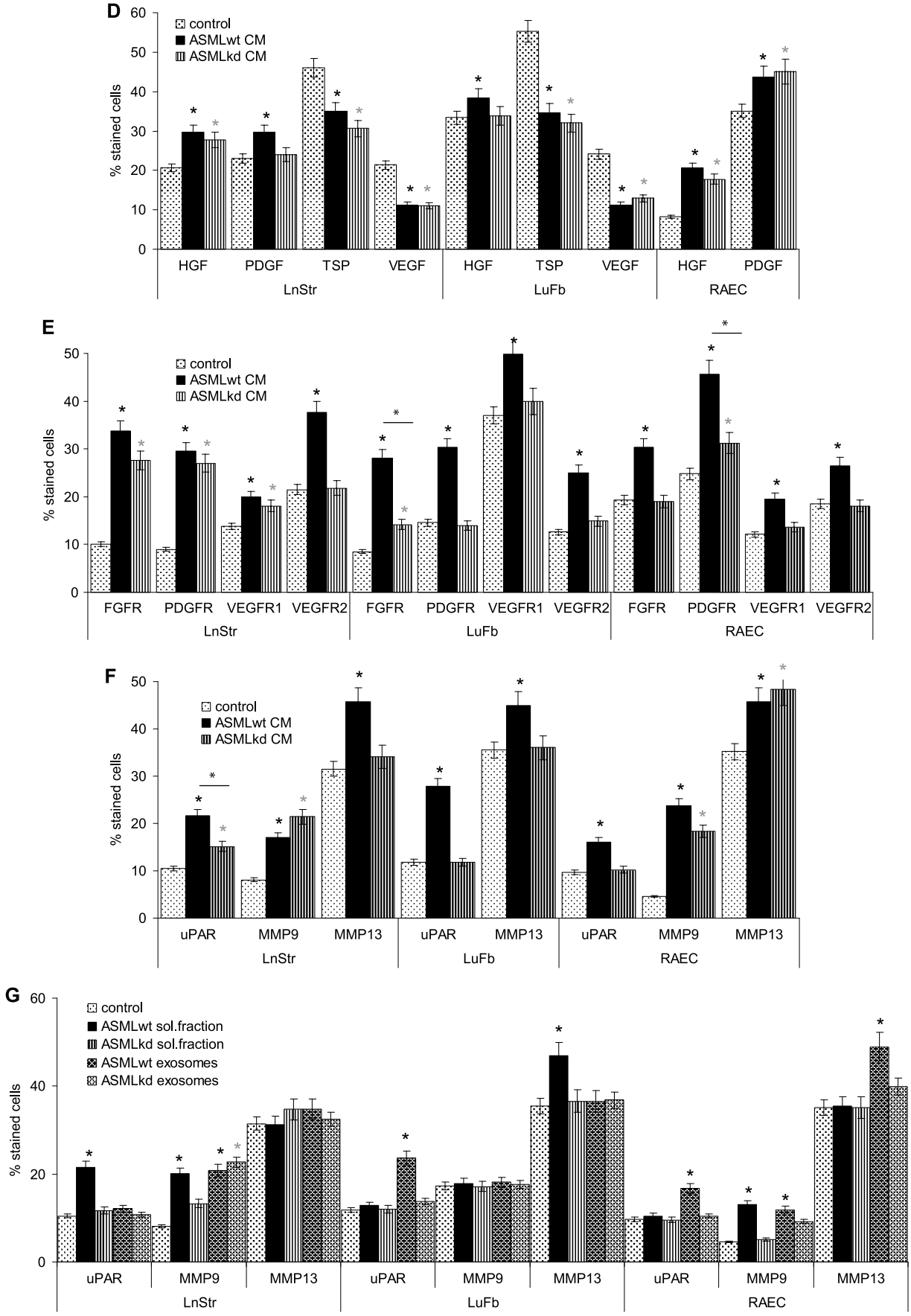

Figure W3. (*continued*).